Missouri S&T Library and Learning Resources

Scholars' Mine

Masters Theses

Student Theses and Dissertations

1973

Neutronics calculations of two fusion reactor blankets

James Edward Struve

Follow this and additional works at: https://scholarsmine.mst.edu/masters_theses

 Part of the Nuclear Engineering Commons

Department:

Recommended Citation

Struve, James Edward, "Neutronics calculations of two fusion reactor blankets" (1973). *Masters Theses*. 3517.
https://scholarsmine.mst.edu/masters_theses/3517

This thesis is brought to you by Scholars' Mine, a service of the Missouri S&T Library and Learning Resources. This work is protected by U. S. Copyright Law. Unauthorized use including reproduction for redistribution requires the permission of the copyright holder. For more information, please contact scholarsmine@mst.edu.

NEUTRONICS CALCULATIONS OF TWO FUSION REACTOR BLANKETS

BY

JAMES EDWARD STRUVE, 1938-

A THESIS

Presented to the Faculty of the Graduate School of the

UNIVERSITY OF MISSOURI-ROLLA

In Partial Fulfillment of the Requirements for the Degree

MASTER OF SCIENCE IN NUCLEAR ENGINEERING

1973

T2850
95 pages
c.1

Approved by

Ioannis Karafoulidis (Advisor) Tom Dolan

James K. Byers

226901

ABSTRACT

At the present state of engineering development, the most probable fusion reactor fuel cycle will use deuterium and tritium in the reaction $^{2}_{1}D + ^{3}_{1}T \rightarrow ^{1}_{0}n + ^{4}_{2}He$. This reaction is exothermic and provides 17.6 Mev of energy of which 14.1 Mev are given to the neutron. The reaction will take place in a plasma environment inside an evacuated chamber. This chamber will be surrounded by a "blanket" which will serve to transform the kinetic energy of the neutron into heat and produce tritium for subsequent use in the fuel cycle. To accomplish this, the blanket will contain materials to slow down and finally absorb the neutron and to produce tritium. The quantity of importance in the production of tritium is the tritium-breeding ratio which is defined as the ratio of tritium atoms produced, divided by tritium atoms consumed. The breeding ratio should be greater than one.

The present work presents calculations of the tritium-breeding ratio and heating rates for two proposed blanket designs. The MONTE CARLO method was used to obtain the results. The materials used for the blanket were vanadium and lithium. Lithium is used to slow down the neutrons and produce tritium by the $^{6}_{3}Li(n,T)^{4}$ He and $^{7}_{3}Li(n,n',T)^{4}_{2}$ He reactions. Vanadium is used as the structural material in the blanket.

Results obtained indicate that a tritium-breeding ratio of 1.3 is easily obtained by either design and that the heating rates for both designs are similar.

ACKNOWLEDGEMENT

This work would not have been possible without the effective guidance of my advisor, Dr. Nick Tsoulfanidis. His insight into the physical processes involved and Monte Carlo simulation techniques were instrumental in the development of a successful simulation. His continuous advice and encouragement are deeply appreciated.

Several other faculty and graduate student members of the Nuclear Engineering Department were of great assistance. Dr. D.R. Edwards was most helpful in providing advice on developing data files. Graduate students Dan Smith and Glenn Schade provided much appreciated assistance in the development of the computer program.

TABLE OF CONTENTS

Table of Contents (Continued) Page

Table of Contents (Continued) Page

LIST OF ILLUSTRATIONS

LIST OF TABLES

I. INTRODUCTION

A. Description of the Problem

Given the present state of engineering development, the most probable fuel cycle for a fusion reactor will be the deuterium-tritium cycle [$D+T \rightarrow \alpha(3.5\ Mev)+n\ (14.1\ Mev)$]. The reactor must be surrounded by a blanket which will produce tritium and transform the kinetic energy of the 14.1 Mev neutron into heat.

The production of tritium is a necessity because tritium is an unstable isotope which decays to He-3 with a 12.33 year half-life. It is generally accepted that the tritium production will be accomplished by a lithium-neutron reaction. Both isotopes of lithium undergo (n,T) reactions. The lithium-6 reaction is exothermic [$Li^7(n,n'T)\alpha+4.78$ Mev] while the lithium-7 reaction is endothermic [$Li^7(n,n'T)\alpha-2.47$ Mev].

In addition to considering the production of tritium in the blanket, the determination of the rate of energy deposition in the blanket and the spatial variation of this deposition are of fundamental importance in designing a fusion reactor.

This work investigates these two parameters, the rate of tritium production per fusion reaction and the rate of energy deposition as a function of the radial distance from the plasma. The reactor is approximated by a quarter section of a right circular cylinder. The Monte Carlo method is used to determine the parameters of interest by following the history of a number of 14.1 Mev neutrons through the blanket. A computer program has been written to perform the necessary computations for the cases analyzed.

The Monte Carlo method was selected because of its geometric flexibility. It has a disadvantage, however, in that the results are probabilistic in nature and have a statistical uncertainty. However, this disadvantage is allayed somewhat by the fact that the uncertainty can be calculated.

B. Review of the Literature

Since an operational fusion reactor has not been built, all investigations of tritium production and energy deposition in the reactor blanket have been done by computer simulation. Several codes which solve the Boltzman equation have been used for these investigations (Ref 1, 2) and two Monte Carlo codes have been used (Ref 3, 4). The Monte Carlo code in Ref 4 has the limitation that it can only consider neutron interactions and does not have the capability of considering the effect of gamma rays on the energy transfer. The code in Ref 3 does not consider any interactions below 1 kev.

Basically two types of blanket configurations have been considered. The more conventional design consists of a vacuum wall surrounding the plasma. Surrounding the vacuum wall is the blanket which typically consists of some fraction of lithium or a lithium compound and some fraction of structural material and a neutron moderating and reflecting material, typically carbon. Steiner (Ref 1) studied this blanket. This will be called the Steiner blanket. The other type of blanket, suggested primarily by R.W. Werner, consists of the blanket surrounding the plasma with

the blanket in turn being surrounded by the vacuum wall. This will be called the Werner blanket.

Neutronics data used for computer codes is taken from Evaluated Nuclear Data File (ENDF-B) information for work done in the United States or equivalent systems in other countries.

C. Need for Present Work

As stated in the preceeding paragraph, numerous studies have been made of the tritium production and energy deposition parameters. The computer codes used for the studies were general codes designed to be used in a variety of situations. As such, certain physical processes were either neglected or dealt with by crude approximations or the geometry used was not representative of the system. The present work, on the other hand, was written specifically to study fusion reactor parameters and takes into account the specific processes of importance in the fusion reactor.

A second need that is met by this work is that it considers vanadium as the vacuum wall and structural material. Most studies to date have used niobium or molybdenum for these components. Vanadium has definite advantages in a fusion reactor in that it does not have as great a proclivity toward nuclear induced gamma radiation as niobium and therefore would not present the radiation hazard in the fusion reactor environment that niobium would. To the author's knowledge, no studies have been done using vanadium as the vacuum wall and structural material.

Finally, to the author's knowledge this is the first comprehensive attempt to study the reactor model proposed by R.W. Werner (Ref 4) which has the vacuum wall located behind the blanket.

II. DEVELOPMENT OF THE COMPUTER PROGRAM FOR THE STUDY OF THE PROBLEM

A. General Description

The Monte Carlo method is a means of studying particle transport by following individual particles as they move through a medium and recording the events that take place. The total of all interactions which happen to a particle during the period it is studied constitutes one particle history.

In effect, the Monte Carlo method simulates a possible experiment that can be performed. In the actual experiment a neutron source, medium and detectors are used to obtain the desired results. In Monte Carlo, this experiment is simulated by the computer as it tracks the individual particles.

In this work, neutrons are assumed to be generated by a source with a space dependence given by a parabola squared distribution. A discussion of this distribution is given in Appendix A. A neutron departs the birth point with an energy of 14.1 Mev and with an equal probability of traveling in any direction from the point of birth; that is, it departs isotropically. The neutron source, i.e., the plasma, is surrounded by a blanket.

The blanket in this work is represented by a series of circular annuli with each annulus representing either a single material or a homogeneous mixture of materials representing the mixture of lithium and structural components in the lithium portion of the blanket.

Because of symmetry and to simplify geometric considerations, the reactor model is represented in the computer program by a

quarter of a cylinder rather than the entire cylinder. This approximation introduces no error into the simulation as the distribution of the neutrons from the plasma is the same in all four quadrants of the cylinder. Additionally, the vertical and horizontal sides of the quarter cylinder are assumed to be completely efficient reflectors. That is, it is assumed that for each neutron that departs the quarter cylinder, another neutron enters the space at the same point and with the same energy but with a different direction. The method used in this case is essentially the same as that used in fission reactor cell calculations.

Neutrons entering the blanket medium can be scattered, absorbed, or, in a limited number of cases (n, 2n reactions), may produce additional neutrons. The type of interaction is determined from the product of the probability of having a neutron interact with a specific type of nucleus and the relative probability that a certain type of interaction will occur between the neutron and the nucleus. A particle history is terminated if a) the neutron is absorbed, b) the neutron leaves the outer surface of the blanket medium, c) the neutron has had 110 interactions and is still inside the medium, or d) the energy of the neutron falls below 1 ev. In the case where the energy falls below 1 ev, the location of the particle is stored and this information is later used by the program to determine what fraction of these neutrons are absorbed in the system by lithium-6 nuclei. A diffusion model approximation is used to determine how many neutrons leak from the wall and moderator into the lithium region. A discussion of this model is contained in Appendix B.

It is felt that this approximation does not introduce serious error into the system. This is because the lithium-6 absorption cross section is several orders of magnitude larger than any other cross section below 1 ev. Further, all absorption cross sections of materials in the blanket have a 1/v dependence below 1 ev so the lithium-6 absorption will continue to be the largest cross section throughout the energy spectrum below 1 ev.

The provision for terminating a history if the number of collisions is greater than 110 is used to avoid unnecessary loss of computer time by studying a history for an indefinite period of time. It does not introduce any significant error into the system as less than 1% of the neutrons studied reached 110 interactions.

To determine whether the neutron has left the blanket, or at what position in the blanket the neutron has had an interaction and produced another particle or deposited energy, the position of the neutron with respect to a fixed coordinate system must be known. To obtain this information, a scheme for tracking neutrons in a fixed cartesian coordinate system has been developed (Ref 5).

In order to reduce the statistical uncertainty of the results obtained by the Monte Carlo method, a total of 3,000 neutron histories were run for each type blanket design studied in this work.

B. Types of Interactions Considered

There are six neutron interactions which are considered in this work. They are:

a) Elastic scattering (n,n)

b) Inelastic scattering (n,n')

c) Absorption (n,γ)

d) $(n,2n)$

e) Tritium production from the lithium-7 isotope $(n,n',T)\alpha$

f) Tritium production from the lithium-6 isotope $(n,T)\alpha$

Each of these interactions is discussed in detail in this section. Charged particle producing reactions such as (n,p) and (n,α) reactions were not considered in this work. The rationale for this decision was that the microscopic cross sections for these reactions were relatively small (less than a millibarn in the energy range of primary interest). Consequently, any statistically significant results would require an excessive number of histories. Finally, gamma ray interactions are discussed.

1. Neutron Elastic Scattering

In elastic scattering, the kinetic energy of the neutron-nucleus system is conserved. By using conservation of energy and momentum one can readily determine the amount of energy given to the scattered neutron and the amount of energy given to the nucleus. The energy given to the nucleus is considered as energy gained by the blanket material.

The relationships for energy and momentum give the following expression for the incident neutron energy loss in the laboratory system (6:168)

$$E' = \frac{1}{2} E[(1+\alpha)+(1-\alpha)\cos\ \theta] \qquad (1)$$

where E' is the energy of the scattered neutron, E is the energy of the incident neutron, $\alpha = [\frac{A-1}{A+1}]^2$ where A is the atomic weight and θ is the polar scattering angle in the center of mass system of coordinates.

In the energy ranges considered in this work, the azimuthal angle, denoted as ϕ, is always considered isotropic. This is not true of the polar angle in both the center of mass (CM) and laboratory systems (LS) of coordinates. The probability of a neutron being scattered through a specific angle between o and π radians in the CM system in a complex function of the incident neutron energy. At higher energies (roughly the Mev energy range), the scattering angle has a definite forward bias. The probability distribution function which represents this forward bias for a given neutron incident energy can be represented by a Legendre polynomial series. In this work, the first four terms of the series were extracted from the ENDF information and they were used to construct this probability function. Using this function, appropriately normalized, the rejection technique (7:145) was used to obtain the polar scattering angle in the CM system. Appendix C contains a discussion of the rejection technique. The angle obtained was then converted to its equivalent value in the laboratory system by the relationship (6:29)

$$\tan \alpha = \frac{\sin \theta}{\frac{1}{A}+\cos\theta} \tag{2}$$

This conversion was required because the coordinate system for the computer program which gives the position of the neutron is the laboratory system of coordinates.

2. Neutron Inelastic Scattering

In inelastic neutron scattering, the incident neutron is absorbed by the target nucleus and subsequently re-emitted, the residual nucleus being left in one of its excited states. The

kinetic energy of the incident neutron is split three ways: The kinetic energy of the emitted neutron, the kinetic energy of the struck nucleus and the excitation energy of the excited nucleus (8:376). This excitation energy will then be emitted as gamma radiation as the nucleus goes to its ground state. The gamma radiation when it is emitted will contribute to the heating of the blanket as will the kinetic energy imparted to the struck nucleus. The transfer of gamma ray energy to the blanket will be discussed in Section B-7 of this chapter.

The determination of the energy given to the nucleus, the emergent neutron and that retained as excitation energy, cannot be achieved by considering the kinematics alone. Most of the nuclei have many levels to which they can be raised by excitation. Therefore, the inelastic event can have more than one outcome. Only for lithium isotopes, which have one excitation level, the outcome is defined by an angle and corresponding energy. As a consequence, two models are used in this work to determine the required energy transfer parameters.

For lithium isotopes, the energy of the scattered neutron, E' is given by (6:214)

$$E' = \frac{E}{(A+1)^2}\left[1+\frac{1}{\gamma^2}+\frac{2\cos\theta}{\gamma}\right] \qquad (3)$$

where E and E' are the laboratory energies of the incident and scattered neutrons respectively, θ is the angle of scattering in the CM system and γ is given by (6:80).

$$\gamma = \frac{1}{A}\sqrt{\frac{AE}{AE-(A+1)\varepsilon}} \tag{4}$$

where ε is the energy of the excitation level of the corresponding lithium isotope.

In the case of the other materials where many levels can be excited, the emergent neutron is no longer given off at a unique energy. In this case, there is a certain probability that the nucleus will be left in one of its excited states and the neutron will have a corresponding energy. When a nucleus has many excited levels, the neutron energy is given by an energy distribution function which is derived with the help of the liquid drop model. In this theory, it is assumed that the neutrons simply "boil off" from the compound nucleus and appear with an energy distribution.

$$N(E')\ dE' = \frac{E'\ \exp\ (E'/T)}{N(T)} \tag{5}$$

where $N(E')\ dE'$ is the probability that the scattered neutron will have an energy between E' and $E' + dE'$. $N(T)$ is a normalization factor and T is the nuclear temperature which is approximately equal to

$$T = 3.22\sqrt{\frac{Em}{A}} \tag{6}$$

Here, Em is the maximum energy available to the scattered neutron, and is given by (6:60)

$$Em = \frac{A}{A+1}\ (\frac{A}{A+1}\ E-\varepsilon) \tag{7}$$

In eqn(7), ε is the minimum excitation level of the nucleus (9:91). Using this model and the rejection technique, the energy of the emergent neutron can be determined.

To determine the energy given to the nucleus for both models, the relationship (9:92)

$$E_{rec} = \frac{A}{(A+1)^2} E + \frac{Em}{A} \tag{8}$$

is used. Here, E is the energy of the incident neutron and Em is maximum energy available to the scattered neutron obtained from equation (7), with the modification that in the multilevel model ε is replaced by Q, the excitation energy given to the nucleus.

In solving eqn(7), Ritts, et al., (9) use the relationship

$$v_r^2 = v_{cm}^2 + v_{rc}^2 \tag{9}$$

where v_r, v_{cm} and v_{rc} represent the speed of the nucleus in the LS, the speed of the center of mass as viewed in the LS and the speed of the nucleus in the CM system, respectively. This assumes that the scattering angle of the nucleus in the CM system is equal to 90 degrees. Since the nucleus is isotropically scattered between 0 and 180 degrees, this represents an average and it should be an adequate approximation for a large number of interactions.

In both models, the neutron is assumed to be isotropically emitted in the CM system. Again, as in elastic scattering, the value for the polar angle in the CM system must be converted into that of the laboratory system; this is accomplished by the relationship (6:29)

$$\tan\mathscr{O} = \frac{\sin\theta}{\gamma+\cos\theta} \tag{10}$$

$$\text{where } \gamma = \frac{\text{Velocity of the center of mass in LS}}{\text{Velocity of the emergent neutron in CMS}} \tag{11}$$

3. Radiative Capture

As stated earlier, the only absorption process (other than those connected with tritium production) which has been considered in this work is radiative capture.

Radiative capture is a relatively unimportant process over much of the neutron energy spectrum concerned since none of the materials considered have a high cross section for radiative capture even for energies approaching the thermal region. Consequently, a very simple model was used for the capture reaction. When a capture reaction occurs, that history is terminated and all the energy of the incident neutron is transferred to the blanket. The model does not allow for gamma radiation to be emitted as a result of the reaction. Since the probability of a capture reaction terminating a history is about .0095 per neutron history, this assumption does not affect the final results significantly.

4. Lithium-6 Tritium Production

The $Li^6(n,T)\alpha+4.78$ Mev reaction is regarded as an absorption reaction and terminates the neutron history. In this reaction the energy of the incident neutron and the 4.78 Mev of energy released as the result of the exothermic reaction are assumed to be given to the blanket at the point of interaction.

5. Lithium-7 Tritium Production

The $Li^7(n,n'T)\alpha-2.47$ Mev reaction differs from the lithium-6 reaction in that there is an emergent neutron, the reaction is endothermic and it has a threshold energy.

Since the reaction is endothermic, the relationship used to determine the energy of the emergent neutron is (10:411)

$$Q = E_3 \left[1 + \frac{M_3}{M_4}\right] - E_1 \left[1 - \frac{M_1}{M_4}\right] - 2\sqrt{\frac{M_1 E_1 M_3 E_3}{M_4}} \cos\theta \qquad (12)$$

where Q = 2.47 Mev, E_1 and E_3 are the incident and emergent neutron energies respectively, M_1 and M_3 represent the neutron mass, M_4 the nucleus mass and θ is the angle of neutron emergence.

The scattering angles ϕ and θ are selected isotropically in the CM system. Again, the polar angle must be converted to the lab system. This is accomplished in the same manner as for inelastic reactions.

6. The (n,2n) Reaction

The (n,2n) reaction is considered proceeding in two steps. First, the incident neutron is inelastically scattered by the target nucleus. Then, if the residual nucleus is left at a virtual level, i.e., with an energy above the binding energy of its least bound neutron, a neutron can escape from the residual nucleus also. The reaction, as would be expected, has a high threshold energy (E_t) which is defined as

$$E_t = \frac{(A+1)}{A} Q \qquad (13)$$

where Q is the binding energy of the least bound neutron in the nucleus (6:60).

It is not clear how other investigators treated the (n,2n) reaction in a Monte Carlo program. The model used in the present work was developed by the author using the evaporation model (11:464)

to determine the energies of the neutrons in the (n,2n) reaction. Conservation of energy and momentum relationships were used to determine the energy imparted to the nucleus. Angles of emission were selected isotropically in the LS. A detailed discussion of the equations involved is given in Appendix D.

Although the nucleus is excited during the reaction, the model assumes that no gamma radiation is emitted and that all excitation energy is carried away by the second neutron. Consequently, the only energy directly imparted to the blanket from the reaction is the recoil kinetic energy of the nucleus.

The parameters of the two neutrons, that is the location of the interaction in cartesian coordinates, the energy of each neutron and the angles giving the direction of motion, are stored in arrays after they are determined. When control is returned to the main program from the (n,2n) model subroutine, the main program then takes the parameters of the last neutron stored by the (n,2n) subroutine, which is the last neutron emitted in the reaction or the secondary neutron, and uses that information to continue the history of the neutron that initiated the (n,2n) reaction until the history is terminated.

Upon termination of that history, the program returns to the data bank. Using the parameters stored for the first neutron, the program generates a new neutron history starting from the point of the (n,2n) interaction. It also increments the number indicating the number of histories to be run by one. This new history is then

followed to termination. After that, the program again checks to determine if there is any information stored in the (n,2n) reaction data bank. If there is none, it starts a new neutron history from the point of birth of the new neutron in the plasma. This check of the (n,2n) reaction data bank is done because of the possibility that a neutron could have more than one (n,2n) reaction during its history. Although this possibility is quite remote, the program is designed to hold the results of five successive (n,2n) reactions.

7. Gamma Ray Interactions

Gamma rays are considered to be produced by two nuclear interactions, radiative capture and inelastic scattering. In this work, the gamma radiation produced by radiative capture is not considered due to the small number of these reactions generated (approximately 1% of the histories are terminated by this type reaction). In the model used in the present work, gamma rays produced by inelastic collisions were produced at a rate about equal to one photon per history. This rate of production is considered important for two reasons. First, the rate of production does have a significant effect on the energy deposited in the blanket. Second, due to the type collision producing these photons, i.e., inelastic, the preponderance of energy is released in areas of the blanket where the neutrons are still quite energetic, that is close to the vacuum wall of the reactor. Since this is the area where most of the heating from other reactions takes place, the effect of gamma ray heating is more critical than if it was spread evenly throughout the entire blanket.

When a gamma ray is generated by an inelastic collision, the energy of the photon and its birth location are stored. After all neutron histories are completed, a subroutine uses the stored parameters of the gamma radiation and gamma ray cross section data stored in the program to determine where the gamma ray's energy is deposited in the blanket.

This determination proceeds in three steps. The first step consists of generating the angle of departure of the photon from the birth point. Isotropic scattering in the laboratory system is assumed. The second step consists of finding the distance from the birth point to the point where the photon has an interaction and gives up energy. The technique used for distance selection is described in Section C-1 of this chapter. If the gamma ray crosses a zone boundary between interactions, this situation is handled in the same manner as discussed in Section D of this chapter. The third and final step in the process consists of depositing some fraction of the gamma ray's energy at the point of interaction. This fraction is obtained by multiplying the gamma energy by the ratio of the absorption cross sections over the total cross section for that photon energy.

After this first collision, the gamma ray history is terminated and the subroutine considers a new particle. Considering only a single interaction is obviously not an excellent approximation. But, this model accounts for most of the gamma ray energy deposited while keeping the required computer time at a minimum. It is the

cost per run which was the deciding factor in holding the number of gamma interactions considered to just one per photon.

C. The Selection Procedure for Distance and Type of Interaction

The distance between interactions, the type of interaction and the scattering angle are all dependent on the neutron cross section. Since the determination of the scattering angle has been discussed in Section B-1 of this chapter, this section will examine the procedures used to select the distance between interactions and the type of interaction.

The neutron cross section used for determining the parameters under discussion are stored as tables in the computer program. The organization of these tables in the computer is discussed in detail in Chapter III. Based on the energy of the incident neutron and the type material the neutron is passing through, the required values of the cross sections are determined by linear interpolation from the appropriate cross section table. The distance between interactions and type of reaction are then determined from these parameters.

1. Selection of the Distance Between Interactions

If the total macroscopic cross section in a given medium is denoted by Σ_t, the probability that an interaction occurs between distance x and x+dx is

$$p(x)dx = \Sigma_t \exp(-\Sigma_t x)dx \tag{14}$$

where p(x) satisfies the following relationship

$$\int_0^x p(x)dx \leq 1, \quad 0 \leq x < \infty \tag{15}$$

This equation can also be expressed as

$$R = \int_0^x p(x)\,dx, \quad 0 \leq R \leq 1 \tag{16}$$

or its equivalent

$$R = \int_0^x \Sigma_t \exp(-\Sigma_t x)\,dx = 1-\exp(-\Sigma_t x). \tag{17}$$

Solving for x gives

$$x = -\frac{1}{\Sigma_t} \ln (1-R) \tag{18}$$

If R is a random number, then 1-R is also a random number. Therefore, an equivalent expression for ln(1-R) is ln(R) and

$$x = -\frac{1}{\Sigma_t} \ln(R) \tag{19}$$

The distance x is selected as eqn(19) indicates. Thus, for a large number of events, the x's selected in this manner will have the exponential distributions given by eqn(14).

2. Selection of the Type of Interaction

If Σ_1, Σ_2 and Σ_3 are nuclear cross sections corresponding to the only possible interactions in a medium, then the total macroscopic cross section in the medium is

$$\Sigma_t = \Sigma_1+\Sigma_2+\Sigma_3 \tag{20}$$

To determine what type of interaction took place, the following steps are used:

a) Select random number R $\mid$ $0 \leq R \leq 1$

b) If $R \leq \frac{\Sigma_1}{\Sigma_t}$, then reaction type 1 occurred

c) If $\frac{\Sigma_1}{\Sigma_t} < R \leq \frac{\Sigma_1+\Sigma_2}{\Sigma_t}$ then reaction type 2 occurred

d) If $R > \frac{\Sigma_1+\Sigma_2}{\Sigma_t}$ then reaction type 3 occurred

The advantage of using this system is that it can be set up to consider a large number of reactions when the selection process is made by a computer program. This was an important consideration in the present work since there are a maximum of 14 different reactions that have to be considered in the blanket.

D. Geometry Considerations

1. General

Two types of reactor configurations are studied in this work. Both have essentially the same general geometry, consisting of a series of concentric cylindrical regions. The regions or zones represent the different type materials or mixtures of materials which make up the blanket of the reactor. These zones may consist of a single material, such as the first vacuum wall which is pure vanadium, or a mixture, such as in the tritium-breeding region, which consists of a structural material, represented in this work by vanadium, and natural lithium (92.44% lithium-7 and 7.56% lithium-6). Figures 1 and 2 show the general geometric configuration of the reactors discussed in this work.

The figures and the computer program only consider a quarter of the cylinder. The quarter cylinder was used for the simulation since it simplified tracking the movement of the neutron. Since the distribution from the plasma is axially symmetric, very little error

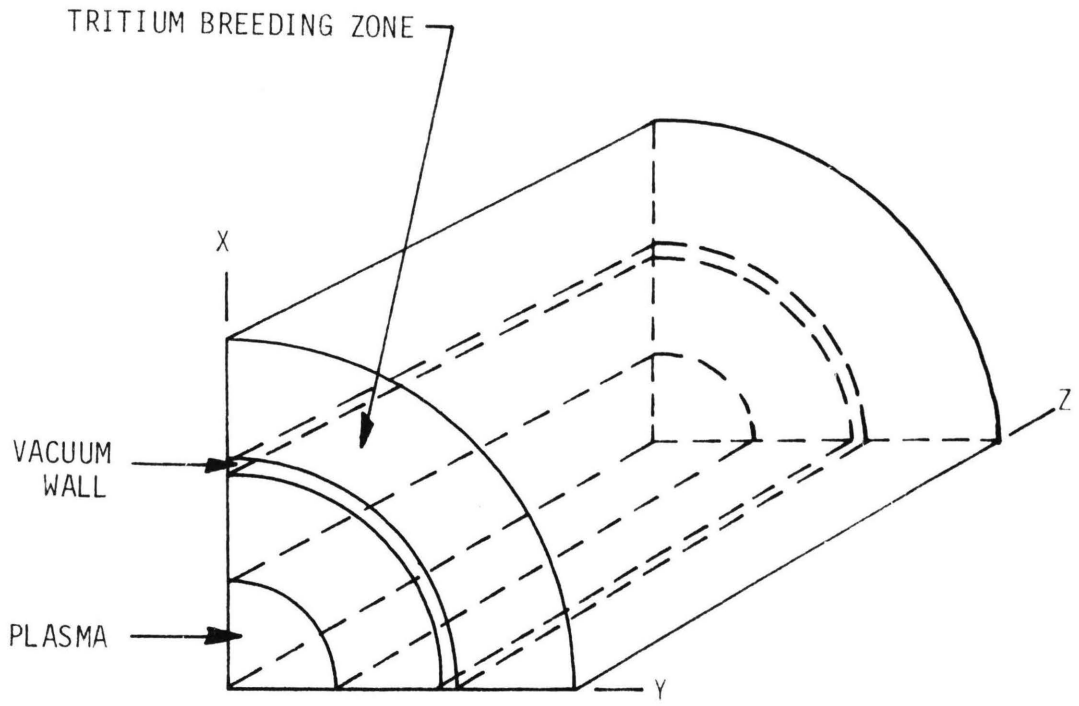

Figure 1 - Geometry Used for the Steiner Blanket Calculations

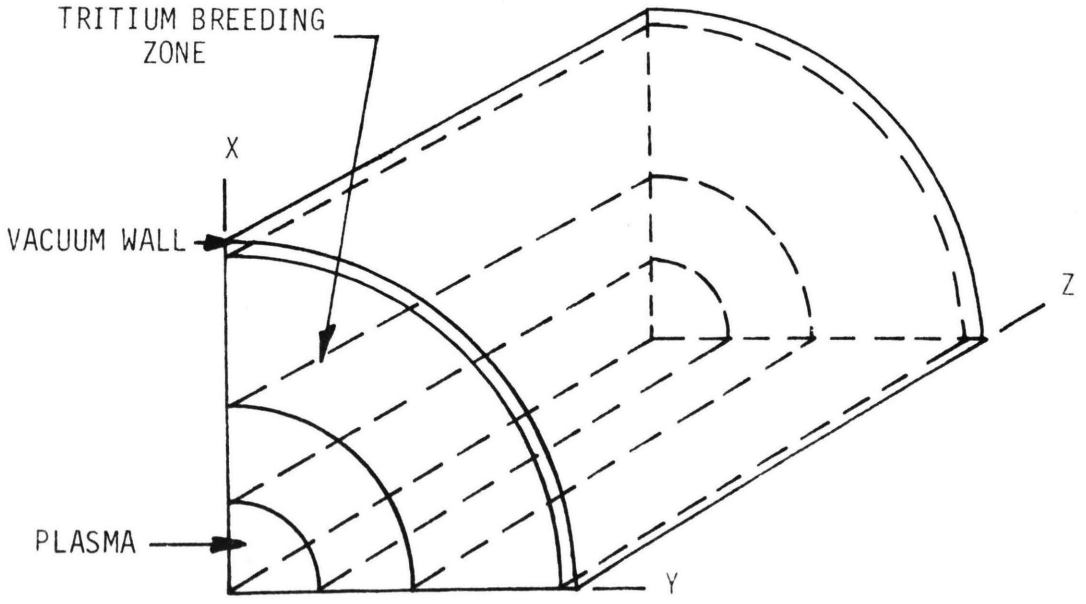

Figure 2 - Geometry Used for the Werner Blanket Calculations

is introduced in the program if the proper boundary conditions are assumed for the quarter cylinder.

2. Boundary Conditions

When a neutron escapes through the outer curved surface of the reactor, it is assumed that it will not return and the history is terminated. In an actual reactor, the outer curved surface would be surrounded by some type of shielding material which would have a finite probability of reflecting the neutron back into the reactor. Since the number and energy of neutrons that cross this boundary is low, this appears to be a good approximation. If a neutron passes through the x-z or y-z plane of the simulated reactor, it is assumed that, because of symmetry, another neutron enters the reactor at the point of departure of the first. In this sense, both the x-z and y-z planes act as perfect reflectors to the neutrons. The path taken by the reflected neutron is shown in figure 3. If it is determined that a neutron has passed through either of the x-y planes representing the ends of the cylinder, again it is assumed to have been reflected back into the simulated reactor. This is done in this case because the length of the cylinder is intended to represent a section of a torus and not a reactor of the mirror machine type. The path taken by this reflected neutron is determined in the way shown by figure 3. The last boundary case considered is if the neutron passes through the initial vacuum wall and back into the plasma region. In this case, rather than trying to determine the angle of reflection from a curved surface, it is assumed that the neutron re-enters the blanket with a new azimuthal angle θ' equal to $180° - \theta$ and a new polar angle ϕ' equal to $180°-\phi$.

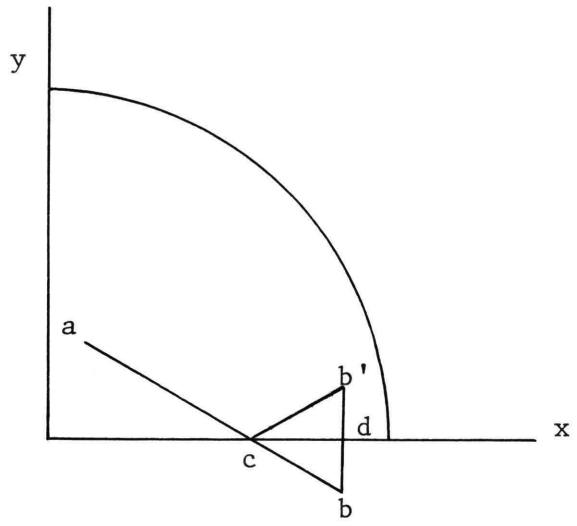

Figure 3 - Reflection From x-z or y-z Plane

Neutron traveling from point a to b is considered reflected at point c and traveling in the direction cb'. Distance cb' is equal to distance cb and angle dcb is equal to angle dcb'.

3. Zone Crossing Points

Since the neutrons are initially very energetic, they normally pass through at least several zones of different compositions before their history is terminated. It is therefore important that the point where a neutron traverses from one zone to another is known so that the proper cross section data can be used.

The subroutine which determines the crossing point is used as part of the particle tracking sequence. The sequence starts with the generation of a distance between interactions and the angles that the neutron travels along this path from a known point. The location of the end of the path is checked against the boundaries of the zone in which the particle started. If the end of the path is between the boundaries of the zone in which the particle started, an interaction is assumed to have taken place in the zone and the type reaction is determined. If the location of the end of the path is outside the zone where the particle started, then the boundary

of the zone has been crossed and the zone crossing point is determined by the subroutine developed for this task. The subroutine is discussed in Appendix E. At the point of zone boundary crossing, a new distance to the next interaction is determined using the parameters of the material in the new zone. The entire cycle is repeated until an interaction takes place or until the history is otherwise terminated. It should be pointed out that when a particle crosses a zone boundary, the direction of the particle and its energy do not change.

III. NUCLEONICS DATA SOURCES

A. Neutron Data

1. Source of Data

Neutron data was obtained from the Evaluated Nuclear Data Files (ENDF). The data was furnished on computer tapes for the files of interest. These tapes were obtained from the National Neutron Cross Section Center (NNCSC), Brookhaven National Laboratory. Since these tapes contained much more data than was required for this work, utility programs (Ref 12) were used to extract the data from the file of interest and put it into a form which was suitable for the program used in this work.

2. Data Extraction

Although nine different data files were obtained from NNCSC, the only files from which data was extracted were carbon, lithium-6, lithium-7 and vanadium. The specific data extracted from the files is shown in table 1.

Table 1 - Data Extracted from Evaluated Nuclear Data Files

	Li-6	Li-7	C	V
Elastic cross section	X	X	X	X
Inelastic cross section	X	X	X	X
Radiative capture cross section	X	X	X	X
Li-6 (n,α)T	X			
Li-7 (n,αn')T		X		
(n,2n) cross section	X	X		X
Angular Dist of Sec. Neutrons	X	X	X	X

3. Storage of Data

The data extracted from the files was interpolated to fit an energy mesh structure (the energy mesh is discussed in Section A-4). In all cases, it was necessary to interpolate between ENDF data points to fill in the energy mesh. The method of interpolation, e.g., linear-linear, linear-logarithmic, etc., was dictated from information contained in the specific data file and by Ref 13.

After the utility programs had extracted the data from the specific data file, a program developed by the author then constructed a table of the neutron parameters of interest for each point in the energy mesh. This table was then read into a magnetic disk where it was stored in the direct-access mode. This process was repeated for each nuclide used.

4. Retrieval of Information

As discussed in the previous paragraph, the data tables constructed for the nuclides used a common energy mesh to set up the cross section data. The original set of data points were those used for the natural iron ENDF/B-II data file. This mesh was fairly fine, consisting of 2998 data points over the range 1 ev to 15 Mev, with the predominance of the points in the range between 1 kev and 1 Mev. This resulted in extremely large data sets, but since the direct access method was used, the data sets were in external storage and caused no high speed core storage problems. In order to obtain a desired cross section, the program determined the two energy index mesh points that bracketed the energy of interest,

read the desired information from the disk from these two energy mesh points and, using a linear-linear interpolation routine, calculated the desired quantity.

Although this system worked well, it was much slower than direct reading from a data table in core storage. Consequently, it was decided to modify the method and read the nuclear data into core storage at execution time. In order to accomplish this, it was necessary to "collapse" the energy spectrum and its associated nuclear data. This was accomplished by making the mesh coarser in the intermediate energy spectrum, i.e., 1 kev to 1 Mev. Using the new energy mesh, cross section data from the initial tables were averaged around the new energy mesh points. The new energy mesh consisted of 437 points which represented a compromise between the desire for a fairly fine mesh and core storage limitations.

The technique used to determine a specific parameter remained the same as in the previous system except that the data was being retrieved from internal storage rather than external storage. This resulted in about a 50% decrease in cycle time for each history.

B. Gamma Ray Data

1. Source of Data

Unlike neutron data, gamma ray data for a nuclide has certain functional relationships with other nuclides.

Because of this and the fact that only two gamma ray parameters, the absorption coefficient and the total attenuation coefficient were needed, the construction of the required data tables was a much simpler task than for the neutron data. In order to construct

the tables, four cross sections were used, compton scattering, compton absorption, pair production and photoelectric effect. Each of these cross sections for a nuclide of interest can be obtained from another nuclide whose cross sections are known by using the following relationships:

a) Photoelectric effect: The relationship for determining the nuclide's photoelectric effect cross section is (10:700)

$$\frac{\tau_1}{\rho_1}\left(\frac{cm^2}{gm}\right) = \frac{\tau_2}{\rho_2}\frac{A_2}{A_1}\left[\frac{Z_1}{Z_2}\right]^n \qquad (1)$$

where τ_1 and τ_2 are the photoelectric cross sections that are desired and known respectively, ρ_1 and ρ_2, A_1 and A_2 and Z_1 and Z_2 are the corresponding densities, atomic weights and atomic numbers of the two materials involved. The exponent n is a function of incident photon energy. For this work, the relationship $n = 4.419+.1614\ \ln(E)$ where E is in Mev, was used to determine n. This relationship was derived from Fig 1.7, p 700, Ref 10.

b) Pair Production: The relationship for determining the pair production cross section is (10:707)

$$\frac{\kappa_1}{\rho_1}\left(\frac{cm^2}{gm}\right) = \frac{\kappa_2}{\rho_2}\frac{A_2}{A_1}\left[\frac{Z_1}{Z_2}\right]^2 \qquad (2)$$

where κ_1 and κ_2 are the pair production cross sections that are desired and known respectively and the other parameters are as defined above.

c) Compton Scattering: The relationship for determining the nuclide's total compton cross section is (10:686)

$$\frac{\sigma_1}{\rho_1}\left(\frac{cm^2}{gm}\right) = \frac{\sigma_2}{\rho_2}\ \frac{A_2}{A_1}\ \frac{Z_1}{Z_2} \qquad (3)$$

where σ_1 and σ_2 are total compton cross sections that are desired and known respectively and the other parameters are as previously defined. The total compton cross section consists of a scattering component and an absorption component. Since the cross section data from which the parameters of interest were to be computed contained only the total compton cross section, it was necessary to use the factors listed on page 29 of Ref 14 which defined the fraction of the cross section that was represented by the absorption component as a function of photon energy.

The known data used was that for aluminum (14:49).

2. Data Table Construction

The data required was extracted from the reference and a computer program was developed to construct data tables. The general setup of the tables is the same as that outlined in the previous section for neutrons. In this case, the energy mesh, which ranged from 10 kev to 15 Mev, was the one contained in Ref 14 for aluminum.

The data tables were constructed, one for wall material (pure vanadium), one for moderator (carbon) and one for the blanket (a mixture of vanadium, lithium-6 and lithium-7).

The total attenuation coefficients and absorption coefficient for the mixture of vanadium and the lithium isotopes were determined from the formula (14:7)

$$\frac{\mu}{\rho} = \sum_i \omega_i \mu_i / \rho_i \qquad (4)$$

where μ_i/ρ_i represents the total attenuation coefficient of the i^{th} material and ω_i is the proportion by weight of the i^{th} material.

Only two values were used in the tables, the total attenuation coefficient, used to determine the distance between interactions and the ratio of absorption cross sections to the total attenuation coefficient. This was used to determine how much of the gamma ray's energy was given to the material in an interaction.

3. Retrieval of Data

The techniques used for retrieving the desired gamma-ray data are essentially the same as that used for neutron data.

Linear-linear interpolation was used again to get the desired cross section data from a given incident photon energy.

IV. RESULTS AND CONCLUSIONS

A. General

The primary neutronics parameters studied in this work are the amount of tritium produced per fusion reaction and the nuclear and gamma heating rates in the blanket. No attempt has been made to include the heating contribution from the plasma radiation even though this radiation could contribute as much as 5% of the thermal output of the reactor (2:89).

1. Tritium-Breeding Ratio: The tritium breeding ratio is defined as the ratio of tritium atoms produced in the blanket to tritium atoms used in fusion reaction. Since each fusion reaction produces one neutron, the breeding ratio in this work is defined as

$$\text{B.R.} = \frac{\text{tritium atoms produced}}{\text{number of histories run}} \qquad (1)$$

2. Heating Rate: In this work, the total heating rate consists of two components; energy given to the nuclei from neutron reactions and energy deposited in the blanket from gamma ray interactions. Again it should be pointed out that the program allows the gamma ray to have only one interaction. Consequently, the heating rates from gamma radiation are lower than they really should be.

The amount of energy deposited in the blanket was measured by dividing the reactor blanket into a series of cylindrical zones approximately one centimeter thick. The program then records the amount of energy stored in each of these zones in units of electron volts. This data is output as a card deck by the program and a second program developed by the author is used to convert the data

to units of watts/cm^3 and to normalize it to the heating rate in each zone per incident neutron. These values can then be multiplied by the number of neutrons incident on the first wall of the blanket in order to determine the heating rate for a given fusion reactor rate.

In this work, the source of 14.1 Mev neutrons was taken to be 10 MW/m^2 incident on the first wall. This is the value used by Steiner in Ref 2.

3. Heat Removal: The majority of the studies of reactor blankets have assumed that the heat generated in the reactor blanket would be removed by pumping the lithium from the blanket through a heat exchanger and then back into the blanket. (Ref 1, 2, 3, 15, 16). Studies concerning the pumping losses involved in this operation have indicated that there may be prohibitive losses incurred by pumping the lithium across the magnetic field lines which contain the plasma (Ref 17, 18).

A solution proposed for this problem is to use some other heat transfer fluid, e.g., helium, which would not be affected by the magnetic field lines (Ref 17, 18). In this work, it is assumed that lithium is not the coolant, but that some other material is used to transfer the heat from the reactor blanket. It is further assumed that the heat transfer fluid is transparent to neutrons; that is, there is essentially no probability of a neutron interaction in the coolant. Using these assumptions, this coolant material is simulated in the present work by introducing a 20% by volume void in the lithium regions of the blanket. This proportion of coolant volume in the

blanket was taken from Werner (Ref 4). No attempt has been made in this work to determine if this volume percent is sufficient to remove the heat generated in the blanket.

B. Results from Steiner Blanket

1. Blanket Design: The blanket studied in this section of the work is based on the design proposed by Steiner in Ref 2. It consists of a vacuum wall surrounding the plasma with the wall being surrounded in turn by a blanket consisting of lithium, structural components and a graphite moderator-reflector. The design parameter for this type blanket are contained in table 2.

2. Neutronics Parameters: Although the total tritium-breeding ratio is considered the parameter of primary interest, seven neutronics parameters are examined in this work. The parameters examined are:

a) B.R. from lithium-6, neutron reactions.

b) B.R. from lithium-7, neutron reactions.

c) Total B.R.

d) Number of neutrons escaping from the blanket.

e) Energy of neutrons escaping from the blanket.

f) Number of radiative capture reactions above 1 ev.

g) Number of (n,2n) reactions in the blanket.

The values obtained from the program for these parameters are contained in table 3. All values listed are normalized to one neutron incident on the vacuum wall. The errors shown are the relative standard errors. The procedure used to determine the errors is contained in Appendix F.

Table 2 - Description of Design-Steiner Blanket

Region Number	Description of Region	Thickness of Region (cm)	Composition of Region Material Volume %	Material Nuclide Density (-24)
1	First wall	0.5	100%V	.7212
2	Lithium and Structure	3.0	6%V 68.5%Li-7 5.6%Li-6	.00433 .03112 .00297
3	Second wall	0.5	100%V	.07212
4	Lithium and Structure	70.0	6%V 68.5%Li-7 5.6%Li-6	.00433 .03112 .00297
5	Moderator-Reflector	60.0	100%C	.08023
6	Lithium and Structure	6.0	6%V 68.5%Li-7 5.6%Li-6	.00433 .03112 .00297

Table 3 - Summary of Tritium-Breeding Results*

Parameter	Value	Relative Error (%)
B.R. from ^{6}Li (n,T)α Reaction	.943	0.45
B.R. from ^{7}Li (n,n'T)α Reaction	.441	2.06
Total B.R.	1.384	0.723
Number Escaping Blanket	.0957	5.39
Energy Escaping (percent of 14.1 Mev)	.144	
Radiative Captures (above 1 ev)	.0090	19.2
(n,2n) Reactions	.0753	6.40

*All values normalized to one incident neutron.

Figure 4 shows the energy spectrum of the escaping neutrons.

3. Heating Parameters: Figure 5 shows the neutron and gamma heating rates for the whole blanket. The discontinuities in the curves represent the change from one type material to another. The lower heating rates are in the carbon moderator where the primary source

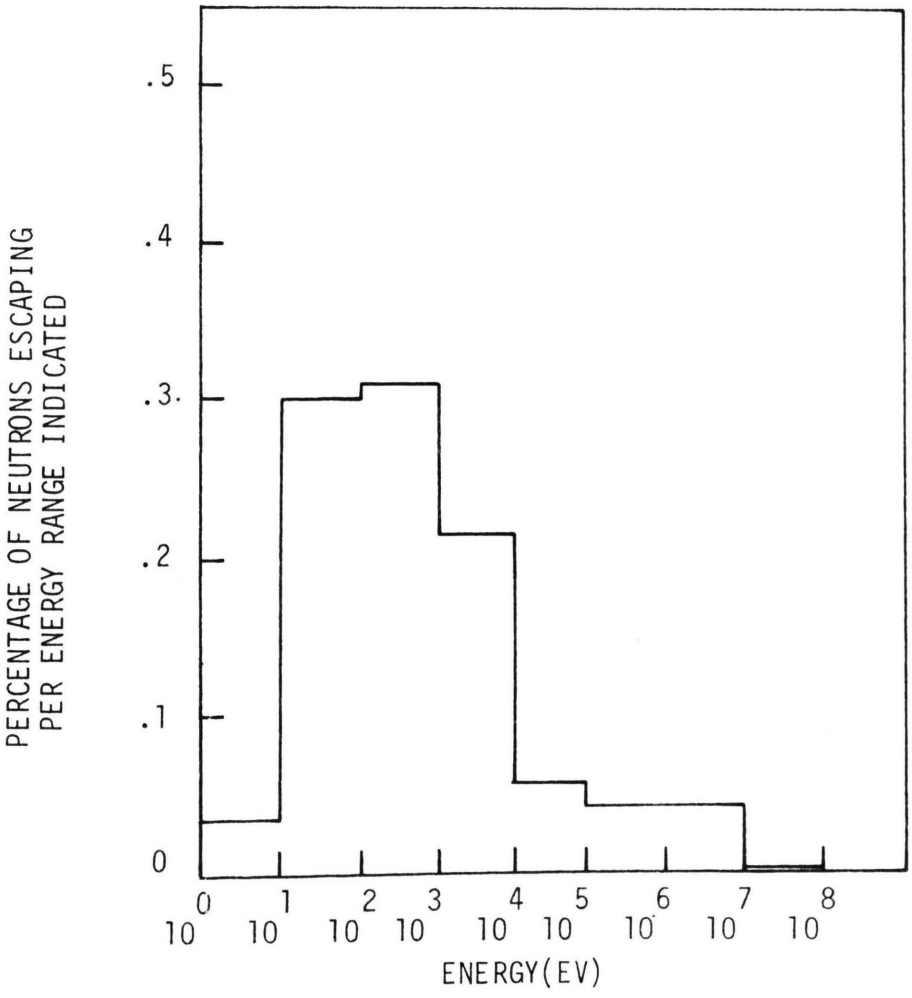

Figure 4 - Energy Spectrum of Neutrons Escaping from Steiner Blanket

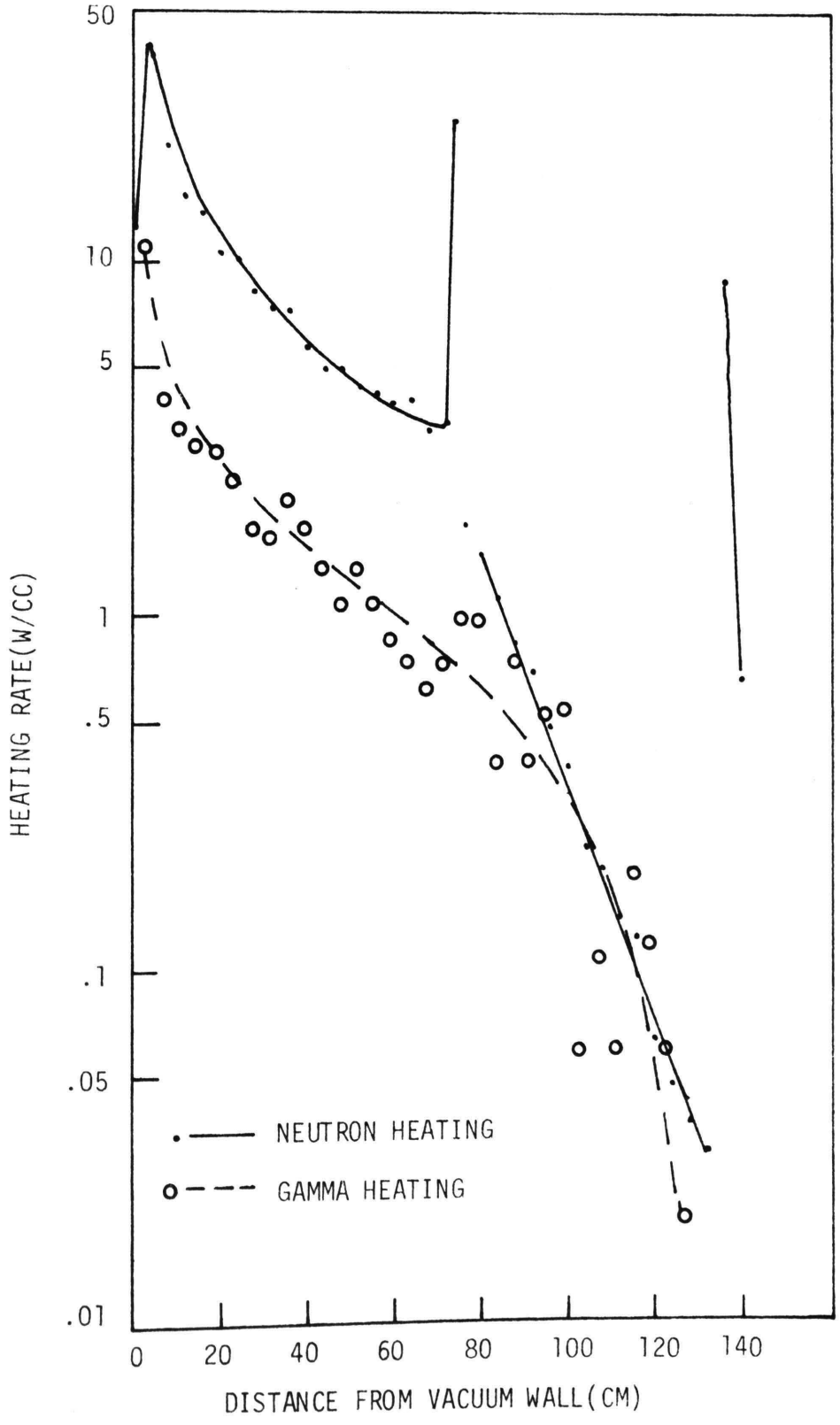

Figure 5 - Neutron and Gamma Heating Rates for Steiner Blanket

of heating is elastic scattering, while the higher heating rates around the moderator reflect the leakage of low energy neutrons from the moderator into the lithium rich portion of the blanket where the exothermic $^{6}Li(n,T)\alpha$ reaction is predominant at low neutron energies.

Tables 4 and 5 contain the numerical values of the points plotted in figure 5 and their relative standard errors. The average error for neutron heating is about 9% with a maximum error of 34.9%. The average error for gamma heating is about 29% with a maximum error of 100.2%. The higher errors associated with the gamma heating results can be attributed to the fact that only a small number of gammas was followed.

4. Comparison with Previous Work: No exact comparison can be made between this and previous works because of the differences in composition, geometry and the method of solution.

With these limitations in mind, the parameters established in this work will be compared to two other studies, one by Steiner (Ref 2) and the other by Blow and his co-workers (Ref 3). Steiner's model of the fusion reactor is, of course, the same as the one examined in this portion of the work. The major variations between this work and Steiner's are: a) this work uses vanadium as the structural material instead of niobium, b) this work uses the Monte Carlo method with a cylindrical geometry while Steiner used a transport theory code with a slab geometry, c) Steiner did not assume void space in the blanket and d) Steiner's blanket is 100 cm. thick while the blanket of this work is 140 cm. Blow and his fellow workers used the same reactor design as Steiner. For their work, however, they used the

Table 4 - Neutron Heating Data for Figure 5

Distance* (cm)	Heating (w/cm^3)	Rel. Error (%)	Distance* (cm)	Heating (w/cm^3)	Rel. Error (%)
0	8.6	5.4	44	4.9	7.7
2	17.8	4.5	46	5.2	7.3
4	43.0	3.3	48	5.0	7.6
6	32.0	3.7	50	4.3	8.4
8	21.8	4.3	52	4.4	8.6
10	18.5	4.5	54	4.2	8.2
12	15.2	4.8	56	4.3	8.2
14	13.7	5.0	58	4.2	8.4
16	13.7	5.1	60	3.9	8.7
18	10.6	5.6	62	3.6	9.3
20	10.4	5.4	64	4.1	8.8
22	9.0	5.8	66	3.5	9.6
24	10.2	5.7	68	3.3	9.8
26	8.8	5.9	70	3.5	9.9
28	8.2	6.1	72	3.5	9.6
30	7.7	6.2	74	25.0	3.7
32	7.4	4.0	76	1.8	4.8
34	7.6	6.3	78	1.6	5.3
36	7.3	6.4	80	1.4	5.1
38	6.9	6.6	82	1.3	5.6
40	5.7	7.1	84	1.1	5.6
42	5.5	7.4	86	.96	6.4

*Distance from Inner Face of Vacuum Wall

Table 4 - Continued

Distance (cm)	Heating (w/cm^3)	Rel. Error (%)	Distance (cm)	Heating (w/cm^3)	Rel. Error (%)
88	.83	6.4	136	8.9	6.1
90	.76	7.9	138	4.6	8.5
92	.69	7.2	140	.64	22.1
94	.49	7.4			
96	.48	8.5			
98	.41	7.7			
100	.37	8.4			
102	.30	9.7			
104	.21	9.8			
106	.22	9.9			
108	.19	13.6			
110	.20	11.8			
112	.14	11.0			
114	.16	14.0			
118	.11	19.9			
120	.061	12.4			
122	.050	13.8			
124	.047	19.3			
126	.071	33.6			
128	.037	14.3			
130	.070	34.9			
132	.031	22.2			
134	20.3	3.6			

Table 5 - Gamma Heating Data for Figure 5

Distance* (cm)	Heating (w/cm^3)	Rel. Error (%)	Distance* (cm)	Heating (w/cm^3)	Rel. Error (%)
0	37.2	8.7	44	1.4	15.9
2	11.6	7.6	46	1.4	17.1
4	11.1	7.4	48	1.1	16.9
6	2.8	12.9	50	1.2	17.9
8	4.4	11.6	52	1.4	17.4
10	3.7	12.1	54	1.2	19.4
12	3.5	11.5	56	1.1	18.3
14	3.3	12.4	58	.90	19.0
16	3.1	12.9	60	.86	22.0
18	3.0	11.9	62	.70	21.8
22	3.1	10.9	66	.82	20.0
24	2.5	13.9	68	.63	24.7
26	2.5	13.5	70	.70	21.7
28	1.8	14.6	72	.75	21.5
30	2.4	12.3	74	.60	24.3
32	1.7	15.4	76	1.0	12.5
34	1.8	15.9	78	.89	19.8
36	2.2	14.1	80	.96	19.7
38	2.2	14.5	82	.82	19.5
40	1.8	15.2	84	.39	27.3
42	1.2	18.8	86	.58	24.2

*Distance from Inner Face of Vacuum Wall

Table 5 - Continued

Distance (cm)	Heating (w/cm^3)	Rel. Error (%)	Distance (cm)	Heating (w/cm^3)	Rel. Error (%)
88	.78	22.3	134	.00	-
90	.26	33.2	136	.00	-
92	.39	32.1	138	.00	-
94	.32	39.0	140	.00	-
96	.52	32.6			
98	.37	33.7			
100	.55	29.3			
102	.37	33.0			
104	.06	72.0			
106	.17	50.9			
108	.11	50.7			
110	.17	45.8			
112	.06	60.0			
114	.09	61.3			
116	.19	50.4			
118	.17	55.7			
120	.12	65.8			
122	.09	58.9			
124	.05	65.0			
126	.02	100.0			
128	.02	100.0			
130	.02	100.0			
132	.00	-			

Monte Carlo method and a cylindrical geometry. The major variations between this work and theirs are: a) they did not compute any heating rates, b) niobium was used as the structural material in their work c) no void area was assumed in the reactor blanket and d) they used a blanket thickness of 100 cm.

Table 6 contains a comparison of some of the tritium-breeding parameters.

Table 6 - Comparison of Tritium-Breeding Parameters*

Parameter	Present Work	Steiner	Blow
B.R. from ^{6}Li (n,T)α Reaction	.943	.90	.875
B.R. from ^{7}Li (n,n'T)α Reaction	.441	.43	.524
Total B.R.	1.384	1.33	1.399
Number Escaping Blanket	.0957	.022	.040
Radiative Capture	.009	.183	.198

*All values normalized to one incident neutron.

As can be seen from this table, the tritium production by lithium-6 for this work is somewhat higher than that obtained by previous works. The explanation for the difference between this work and that of Blow can probably be attributed to the fact that his work did not consider low energy neutron reactions, where the probability of a tritium producing lithium-6, neutron reaction is higher. The variation between Steiner's work and this one is not so easily explained. It is probable that the geometry used and/or the different method of solution contributes to the difference.

The probability of a neutron escaping the blanket is another area where a variation occurs. This could be caused by two factors.

First, as can be seen from the radiative capture rates, the loss through parasitic absorption is much smaller for the present work because of the use of vanadium instead of niobium as the structural component of the reactor. A second factor is the lower nuclide density of the materials in the present work due to the introduction of the voids in the system. This lower density should result in smaller macroscopic cross sections, hence, lower reaction rates and an increased probability of leakage.

As stated previously, only Steiner has published heating calculations for reactor design considered in this section. Comparisons of the neutron and gamma heating rates are contained in table 7. Since the thickness of the two blankets are different, the points of comparison are picked to be at the same relative location in the two blankets, e.g., the center of the moderator reflector, to increase the validity of the comparison.

Table 7 - Comparison of Heating Rates (watts/cm^3)

	Neutron Heating		Gamma Heating	
Location	Present Work	Steiner Work	Present Work	Steiner Work
A	8.6	120.0	37.2	9.0
B	21.9	45.0	4.6	8.5
C	43.0	40.0	11.13	7.2
D	5.7	11.0	1.8	3.0
E	3.5	6.5	0.6	1.1
F	0.30	1.2	0.365	0.6
G	0.638	1.05	0.0	0.35

Location of Points Used in Table 7

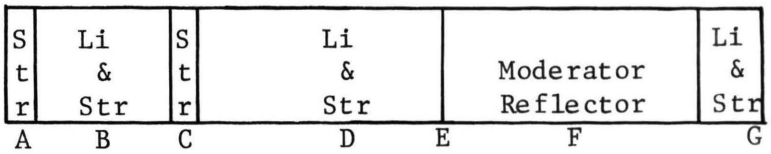

Location	Description
A	Inner vacuum wall face
B	Center of vacuum wall structure
C	Beginning of 1st lithium blanket zone
D	Center of 1st lithium blanket zone
E	End of 1st lithium blanket zone
F	Center of carbon moderator
G	End of 2nd lithium blanket zone

As can be seen from this admitedly rough comparison, the rates are quite similar except in the area of the vacuum wall. The cause or causes of the differences of the heating rates in the vicinity of the vacuum wall cannot be stated with any precision because of the differences in materials and the method of solution. Both of these factors could contribute to the differences observed. From the material standpoint, the macroscopic total cross section of niobium is about 30% higher than that for vanadium at 14.1 Mev based on ENDF data. A higher probability for interaction in this area would, of course, result in a higher heating rate. This would be particularly true in the wall area which has a higher proportion of structural material than the other parts of the reactor. Steiner used transport theory and slab geometry. The Monte Carlo method simulates more accurately both geometry and the occurrence of possible

events. It is unfortunate that Blow and his co-workers did not do heating calculations in their study as this would have given an indication of what effects the different type solutions have on the results. As it stands now, it is only possible to offer possible causes for the differences in the two results, but not quantified estimates of what their effect is.

C. Results from Werner Blanket

1. Blanket Design: The blanket studied in this section of the work is based on the design proposed by Werner in Ref 4. It consists of a blanket containing lithium and structural components closest to the plasma. The blanket is then surrounded by the vacuum wall. Vanadium is used as the structural material in this work. The design parameters for this fusion blanket are contained in table 8.

Table 8 - Description of Design-Werner Blanket

Region Number	Description of Region	Thickness of Region (cm)	Composition of Region: Material Volume %	Composition of Region: Material Nuclide Density (-24)
1	Blanket wall	1 m.m.	100%V	.07212
2	Lithium and Structure	190 cm	6%V 68.5%Li-7 5.6%Li-6	.00433 .03112 .00297
3	Vacuum wall	2 cm	100%V	.07212

2. Neutronics parameters: The seven parameters examined are:

a) B.R. from $^{6}Li(n,T)\alpha$ Reaction

b) B.R. from $^{7}Li(n,n'T)\alpha$ Reaction

c) Total B.R.

d) Number of neutrons escaping from blanket

e) Energy of neutrons escaping from the blanket

f) Number of radiative capture reactions above 1 ev

g) Number of (n,2n) reactions in the blanket

The values obtained from the program for these parameters are contained in table 9. All values listed are normalized to a value of one neutron incident on the blanket wall. The errors shown are the relative standard errors. The procedure used to determine the errors is contained in Appendix F.

Table 9 - Summary of Tritium-Breeding Results*

Parameter	Value	Relative Errors (%)
B.R. from ^{6}Li (n,T)α Reaction	.870	.71
B.R. from ^{7}Li (n,n'T)α Reaction	.484	1.88
Total B.R.	1.354	.81
Number Escaping Blanket	.163	4.14
Energy Escaping (percent of 14.1 MeV)	1.95	
Radiative Capture	.0217	12.2
(n,2n) Reactions	.0543	7.62

*Values are normalized to one incident neutron.

Figure 6 shows the energy spectrum of the neutrons escaping from the reactor.

3. Heating Parameters: Figure 7 shows the neutron and gamma heating rates for the blanket. The discontinuities in the curves are caused by the different reactions and reaction rates in the blanket and the vacuum wall. Tables 10 and 11 contain the numerical values of the points plotted in figure 7 and their relative standard errors. The average error for neutron heating is about 10% with a maximum error of 27.3%. The average error for gamma heating is

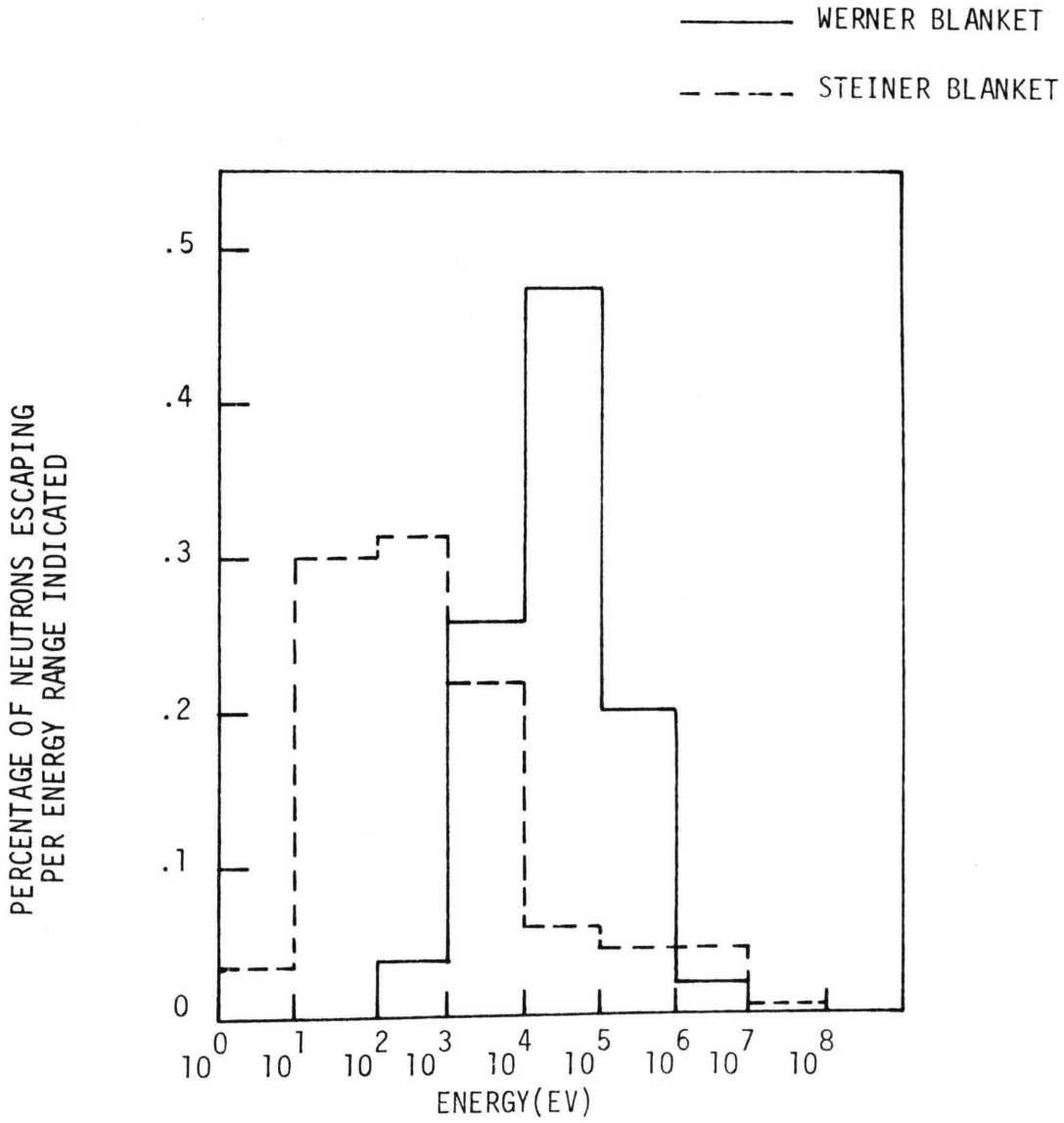

Figure 6 - Energy Spectrum of Neutrons Escaping from Werner Blanket Compared to Steiner Blanket

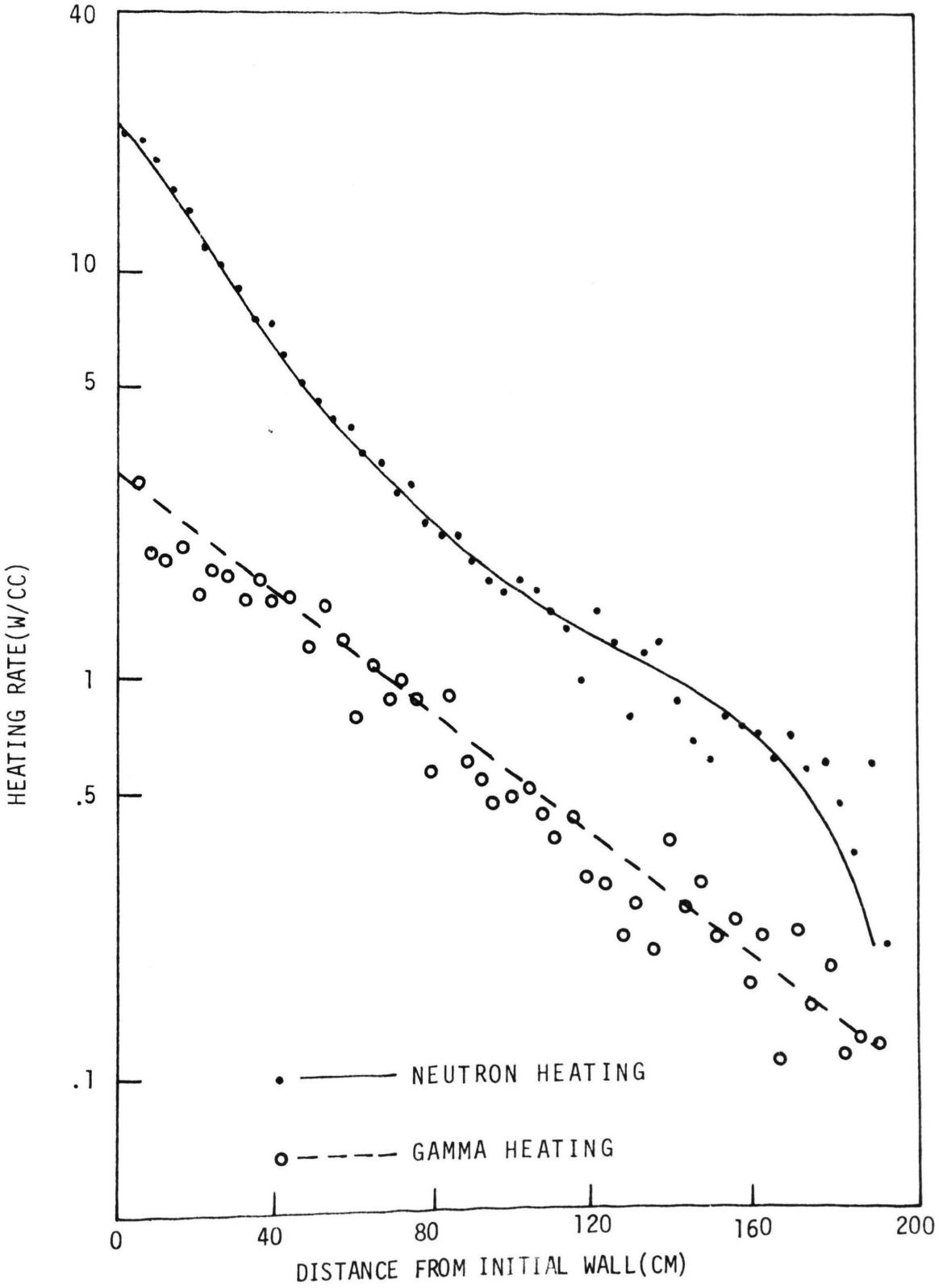

Figure 7 - Neutron and Gamma Heating Rates for Werner Blanket

Table 10 - Neutron Heating Data for Figure 7

Distance* (cm)	Heating (w/cm^3)	Rel. Error (%)	Distance* (cm)	Heating (w/cm^3)	Rel. Error (%)
0	22.3	6.6	84	2.3	9.2
4	21.2	3.3	88	2.0	10.0
8	19.0	3.3	92	1.7	10.1
12	16.2	3.5	96	1.7	10.5
16	14.4	3.7	100	1.8	10.4
20	11.7	4.0	104	1.6	10.6
24	10.6	4.1	108	1.5	11.4
28	9.0	4.4	112	1.3	11.9
32	7.0	4.8	116	.96	13.6
36	7.7	4.9	120	1.5	11.9
40	6.3	5.2	124	1.2	12.4
44	5.5	5.9	128	.79	15.0
48	4.8	5.9	132	1.1	12.7
52	4.4	6.4	136	1.2	12.2
56	4.2	6.4	140	.86	14.2
60	3.6	7.0	144	.70	16.0
64	3.5	7.1	148	.60	16.8
68	2.9	7.8	152	.79	15.0
72	3.0	7.7	156	.76	15.3
76	2.4	8.6	160	.74	15.5
80	2.3	8.7	164	.63	16.5

*Distance from Inner Face of Blanket Wall

Table 10 - Continued

Distance (cm)	Heating (w/cm^3)	Rel. Error (%)
168	.72	15.5
172	.58	17.0
176	.61	16.6
180	.49	18.4
184	.36	21.3
188	.62	16.3
192	.20	27.3

Table 11 - Gamma Heating Data for Figure 7

Distance* (cm)	Heating (w/cm^3)	Rel. Error (%)	Distance* (cm)	Heating (w/cm^3)	Rel. Error (%)
0	7.0	13.9	84	.94	14.6
4	3.4	9.5	88	.66	15.9
8	2.1	11.7	92	.59	16.0
12	2.1	12.1	96	.51	19.1
16	2.2	11.1	100	.52	20.0
20	1.7	12.0	104	.56	17.9
24	1.9	11.7	108	.48	19.4
28	1.9	11.6	112	.44	20.0
32	1.6	12.4	116	.47	19.5
36	1.8	11.0	120	.34	19.4
40	1.6	12.3	124	.32	20.8
44	1.6	11.6	128	.24	23.5
48	1.2	14.1	132	.29	23.0
52	1.5	12.0	136	.21	26.3
56	1.3	12.3	140	.42	20.3
60	.82	14.6	144	.29	22.1
64	1.1	13.6	148	.33	21.5
68	.94	15.8	152	.24	25.9
72	1.0	14.5	156	.26	24.1
76	.94	14.2	160	.18	28.2
80	.60	18.0	164	.24	24.0

*Distance from Inner Face of Blanket Wall

Table 11 - Continued

Distance (cm)	Heating (w/cm^3)	Rel. Error (%)
168	.12	33.8
172	.24	22.9
176	.16	29.7
180	.19	28.2
184	.12	28.4
188	.13	32.8
192	.12	33.8

about 19% with a maximum error of 33.8%. As mentioned in the previous section, the higher error associated with the gamma heating results can be attributed to the fact that a small number of gammas was followed.

4. Comparison with Previous Work: Only one work, that of Werner, has examined the design discussed in this section. The major differences between this work and Werner's concerns the choice of structural material and the types of heating considered. Werner, in his work, used niobium as the structural material. His heating calculations consider only total heating since the Monte Carlo code he used does not have the capability of considering gamma interactions. The present work uses vanadium as the structural material and does consider gamma heating. Werner's results for tritium-breeding consider that a 20% void exists in the blanket to represent the coolant.

Table 12 contains a comparison of the tritium-breeding parameters which were computed in both works. Werner did not present data on the number of (n,2n) or radiative capture reactions, nor on the fraction of neutrons escaping.

Table 12 - Comparison of Tritium-Breeding Parameters

Parameter	Present Work	Werner's Work
B.R. from ^{6}Li (n,T)α Reaction	.87	.753
B.R. from ^{7}Li (n,n'T)α Reaction	.484	.807
Total B.R.	1.354	1.560

As can be seen from the table, the B.R. results from lithium-6 reactions are in fair agreement, the present works being about 16%

higher than Werner's results. The B.R. results for lithium-7 are in poorer agreement, i.e., Werner's results are about 67% higher than the present work's results. Since the $^{7}Li(n,n'T)$ reaction has a threshold energy for the reaction of 2.52 Mev, this would indicate that the neutrons remained at a higher energy through more collisions in Werner's model in order to have the higher number of tritons produced from lithium-7 interactions. The reason for the neutrons remaining at a higher energy is not immediately obvious. It could possibly be related to the difference in structural material or it could be caused by the manner in which the codes treat a specific reaction. Neither of these factors, it would seem, should be sufficient to cause the difference between the two results.

A comparison of the heating rates for this work and Werner's is contained in figure 8. In this case, the total heating rates are compared since this is how Werner presented his data. As can be seen from the figure, the slopes of the curves are similar; however, the rates are higher for Werner's work. There are three probable explanations for this. First, the code used by Werner, SORS-N, does not consider gamma contributions at all. If a gamma-ray producing reaction, e.g., an inelastic reaction, is determined to have happened at a location in the blanket, the energy deposited at that point is assumed to be the total energy of the incident neutron. This should result in comparatively higher heating rates for Werner's results since the present work does not take into account all the heating that

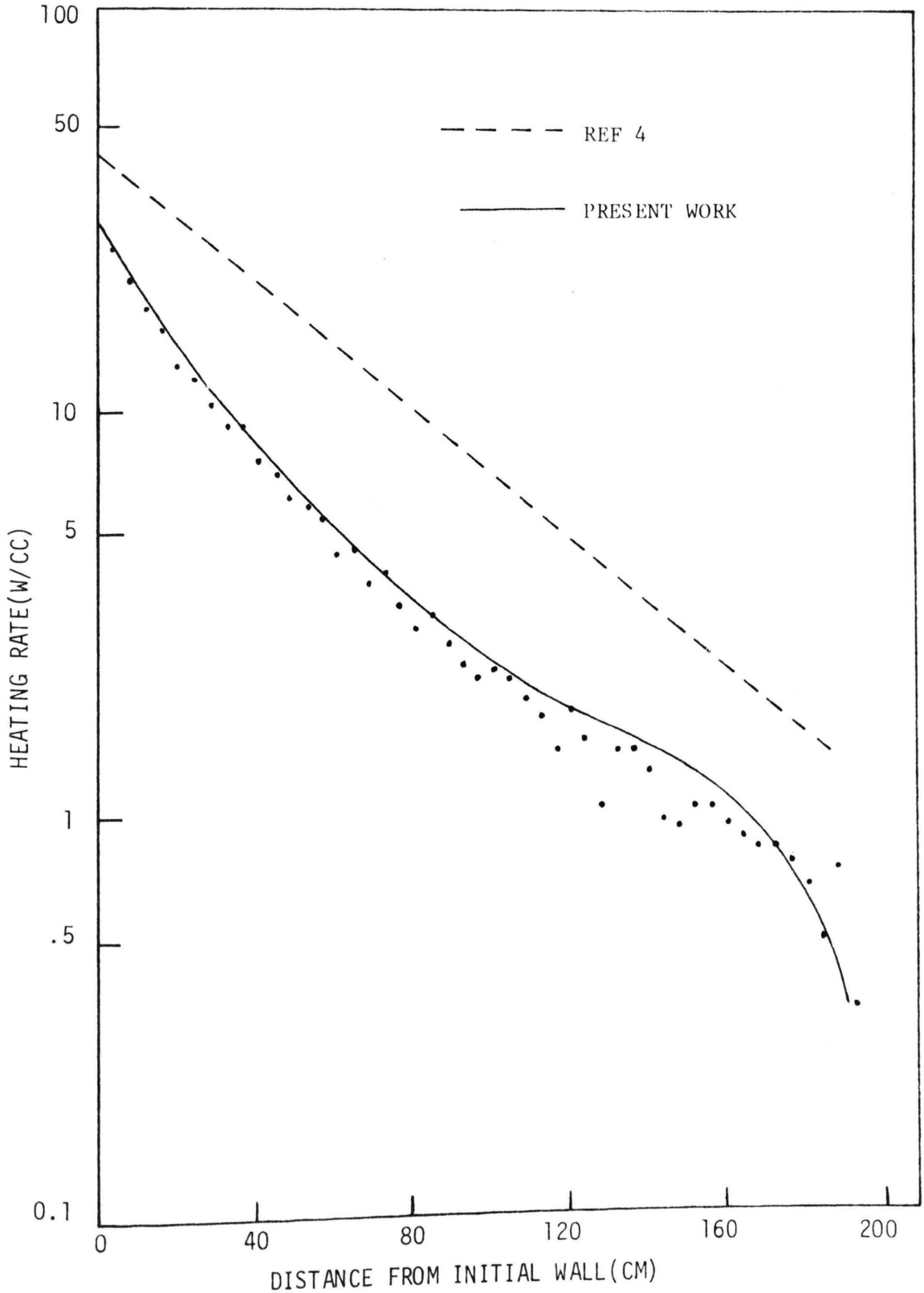

Figure 8 - Comparison of Total Heating Rates Determined in Present Work with Those Determined by R.W. Werner

would be caused by gamma radiation. Second, the use of niobium should affect the results. Finally, for his heating studies, Werner assumed a blanket composition that was a homogeneous mixture of 95% natural lithium and 5% niobium and no voids. This denser blanket should also result in higher heating rates because the probability of an interaction in a unit volume will be increased with the increased nuclide densities.

D. Conclusions

This work has achieved its objective of calculating the tritium-breeding ratio and heating rates for a fusion reactor blanket. The values obtained are in general agreement with previous results. However, the lack of published results using the specific materials that were used in this work makes it difficult to reduce the comparison to quantitative terms.

A comparison of the results obtained by this work for the two types of fusion reactor blanket designs indicates that the neutronics parameters are quite similar. It appears that the blanket proposed by Steiner is superior to that of Werner in the area of heat generated per unit volume. This may be illusory, however, as the Werner model has the capability, because of its design, to allow a higher flux of neutrons to impinge on the wall of the blanket. This would result in higher power densities, and that fact, coupled with the maintenance advantages presented by Werner's proposed design would indicate that the design could be superior to that proposed by Steiner. Based on

this work, however, the only conclusion that can be drawn is that the neutronics parameters indicate no clear superiority for either design and that other parameters will have to be investigated to determine if one design is clearly superior.

E. Recommendations for Further Work

This investigation has been a rather limited study of tritium-breeding ratios and heating rates for two types of fusion reactor blankets. The program used for this study has the potential for studying other situations with little modification. Recommended areas for further work are:

1. Gamma Heating: The model used to determine gamma heating rates is an over-simplified model. To improve the results obtained for this parameter, the subroutine which computes the heating rates could be modified to allow more than one interaction for the gamma history. Alternatively, the location, energy and direction of motion of the gamma ray could be output and used in another program such as the one developed by Kuspa (Ref 19).

2. Use of Other Materials: Comparisons between the results obtained in this work and that of previous works were handicapped by the fact that different materials were used. Use of other materials such as niobium, molybedenum and flibe would allow more realistic and varied parameter studies with the program. Use of these new materials would require the preparation of new data files from the ENDF tapes that could be accepted by the program.

3. Shielding Studies: To determine the worth of a particular design, the shielding requirements should be considered. Extending

the program to consider the shielding aspects would involve obtaining the required Evaluated Nuclear Data Files, preparing them to be accepted by the program and a limited modification of the program to accept the increased number of materials.

4. Increasing the Efficiency of the Program: The primary effort in this work was to approximate the physical system. Consequently, much of the effort was directed to developing models which approximated the specific nuclear reactions. As a result, the Monte Carlo techniques used are not very sophisticated and the time used to obtain an adequate sample is quite large (about 50 minutes on the IBM 360-50 for 3000 histories). By using more sophisticated techniques, it should be possible to reduce the time required to obtain an adequate sample.

BIBLIOGRAPHY

1. Steiner, D. "Nuclear Performance of Fusion Reactors," Nuc. Appl. & Tech. 9, 83 (1970).

2. Steiner, D. "Neutronic Behavior of Two Fusion Reactor Blanket Designs," B.N.E.S. Nuclear Fusion Conference, 483 (1969).

3. Blow, S., Crocker, V. and Wade, B. "Neutronics Calculations for Blanket Assemblies of a Fusion Reactor," B.N.E.S. Nuclear Fusion Conference, 492 (1969).

4. Werner, R. "Module Approach to Blanket Design - A Vacuum Wall Free Blanket Using Heat Pipes," B.N.E.S. Nuclear Fusion Conference, 536 (1969).

5. Tsoulfanidis, N. Private Communication. April 1972.

6. Lamarsh, J. Introduction to Nuclear Reactor Theory. Reading, Massachusetts: Addison-Wesley Publishing Company, Inc., 1966.

7. Clark, F. Advances in Nuclear Science and Technology, Henly, E. and Lewins, J., Ed., Vol 5, New York: Academic Press (1969).

8. Fitzgerald, J., Brownell, G. and Mahoney, F. Mathematical Theory of Radiation Dosimetry, New York: Gordon and Breach Science Publishers, Inc. (1967).

9. Ritts, J.J., et al., "Calculation of Neutron Fluence-to-Kerma Factors for the Human Body," Nuc. Appl. & Tech. 7, 89 (1969).

10. Evans, R. The Atomic Nucleus, New York: McGraw-Hill Book Company, 1955.

11. Odette, G. "Energy Distribution of Neutrons from (n,2n) Reactions," ANS Transactions 15, 464 (1972).

12. Jenkins, J. "RICE: A Program to Calculate Primary Recoil Spectra from ENDF/B Data." U.S.A.E.C. Report ORNL-TM-2706, Oak Ridge National Laboratory (1970).

13. Drake, M., Ed. "Data Formats and Procedures for the ENDF Neutron Cross Section Library," BRL 50274, Brookhaven National Laboratory, (1970).

14. Hubbell, J. "Photon Cross Sections, Attenuation Coefficients, and Energy Absorption Coefficients from 10 kev to 100 Gev," NSRDS-NBS 29, National Bureau of Standards, (1969).

15. Borgwaldt, H., et al., "Neutronics and Thermal Design Aspects of Thermonuclear Fusion Reactor Blanket," Proceedings of the Fourth International Conference on Plasma Physics and Controlled Nuclear Fusion Research, Vol III, 457 (1971).

16. Lee, J. "Tritium Breeding and Energy Generation in Liquid Lithium Blankets," B.N.E.S. Nuclear Fusion Conference, 471 (1969).

17. Forster, S. "Blanket Cooling Concepts and Heat Conversion Cycles for Controlled Thermonuclear Reactors," Proceedings of the Fourth International Conference on Plasma Physics and Controlled Nuclear Fusion Research, Vol III, 469 (1971).

18. Hopkins, G., and Melese-d'Hospital, G. "Direct Helium Cooling Cycle for a Fusion Reactor," B.N.E.S. Nuclear Fusion Conference, 552 (1969).

19. Kuspa, J. "Calculation of Buildup Factors for Multi-Layer Slab Shields Using the Monte Carlo Method," Masters Thesis, University of Missouri-Rolla (1972).

20. Irving, D., Cain, V. and Freestone, R. "An Amplification of Selected Portions of the 05R Monte Carlo User's Manual," ORNL-TM-2601, Oak Ridge National Laboratory (1969).

21. Spanier, J., and Gelbard, E. Monte Carlo Principles and Neutron Transport Problems. Reading, Massachusetts: Addison-Wesley Publishing Company, Inc., 1969.

22. Abramowitz, M., and Segun, I., Ed., Handbook of Mathematical Functions. New York: Dover Publications, Inc., (1965).

23. Abdou, C., and Maynard, C. "Neutron Source Geometry Effects on Fusion Reactor Blankets," ANS Transactions 15, 34 (1972).

24. Clark, M., and Hansen, K. Numerical Methods of Reactor Analysis. New York: Academic Press, Inc., 1964.

25. Glasstone, S., and Loveberg, R. Controlled Thermonuclear Reactions. New York: Von Nostrand Reinhold Company, Inc., (1960).

26. Kimlinger, J., and Plechaty, E. "SORS Monte Carlo Neutron Transport Code for the CDC-6600," UCRL-50532, Lawrence Radiation Laboratory (1968).

27. Lederer, C., Hollander, J., Perlman, I. Tables of Isotopes. New York: John Wiley and Sons, Inc., (1967).

28. Poenitz, W. "The Black Neutron Detector," ANL-7915, Argonne National Laboratory, (1972).

29. Pearlstein, S. "Analysis of (n,2n) Cross Sections for Medium and Heavy Nuclei," Nuc. Sci. & Engr. 23, 238 (1965).

VITA

James Edward Struve was born in Columbus, Nebraska, on February 4, 1938. He received his primary and secondary education in Seward, Nebraska. He attended the United States Military Academy at West Point, New York, receiving a Bachelor of Science degree in June 1961. Since graduating from the Academy, he has been on active duty as an officer in the United States Army. He has been enrolled in the Graduate School of the University of Missouri-Rolla since January 1971.

Appendix A - Distribution of Neutrons Born in Plasma

In Ref 23, the authors suggest that the analytical expression that best describes the spatial distributions of D-T reactions in a plasma is a parabola squared distribution function. This function can be represented by the relationship

$$p(x) = (xm^2 - rx^2)^2 \tag{1}$$

where xm is the radius of the plasma and rx is the radial distance from the center of the plasma. The location of the birth point of the neutron in the x-y plane is obtained by using the rejection technique with a normalized form of eqn(1):

$$p(x) = \left(\frac{xm^2 - rx^2}{xm^4}\right)^2 \tag{2}$$

Figure 9 shows the distribution function denoted by eqn(2):

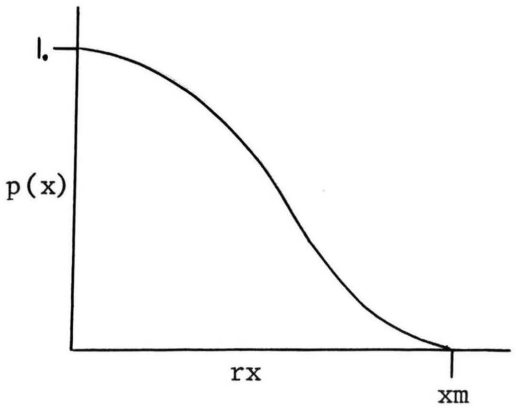

Figure 9 - Neutron Distribution Function

The location of the birth point in the z direction is obtained by multiplying the length of the cylinder by a uniformly distributed random number.

Appendix B - Treatment of Neutrons with Energies Below 1 ev

The lowest energy limit for the Monte Carlo portion of the program is 1 ev. If the neutron energy is less than that value after an interaction, a diffusion equation approximation is used to determine how many neutrons below 1 ev will leak out of the vanadium walls and carbon moderator into the lithium blanket and be absorbed by the lithium. The reactor is assumed to have an infinite slab geometry for this model. It is further assumed that once the neutrons leak out of the wall or moderator they do not return.

In this case, the diffusion equation

$$\frac{d^2\phi}{dx^2} - \frac{\phi}{L^2} = \frac{S}{D} \qquad (1)$$

is used where ϕ is the flux, L the diffusion length, D the diffusion coefficient and S is the source. The value of S is equal to the number of neutrons found to be below one electron volt in the zone of interest, e.g., the moderator zone. Solving the diffusion equation gives

$$\phi(x) = \frac{S}{\Sigma_a} + A \cosh(x/L) + C \sinh(x/L) \qquad (2)$$

Assuming the distribution of the neutrons to be symmetrical, C is set equal to zero to meet the symmetry boundary condition. Using the boundary condition that the flux goes to zero at the extrapolated distance, defined as $a/2$, gives the equation

$$\phi(a/2) = 0 = \frac{S}{\Sigma_a} + A \cosh(a/2L) \qquad (3)$$

solving this equation for A gives

$$A = \frac{-S}{\Sigma_a} \frac{1}{\cosh\ (^a/2L)} \tag{4}$$

and a value for the flux of

$$\phi(x) = \frac{S}{a} [1 = \frac{\cosh\ (^x/L)}{\cosh\ (^a/2L)}] \tag{5}$$

The number of neutrons absorbed in a particular zone is equal to

$$\int_{b/2}^{b/2} \phi(x)\ \Sigma_a dx \tag{6}$$

where b/2 is the actual boundary of the zone. Substituting the value of the flux determined above into this equation and integrating gives

$$\text{number of absorptions} = S\ [^{b-2\ \sinh\ (^b/2L)}_{\cosh\ (^a/2L)}] \tag{7}$$

The number leaking out of the slab is equal to the number of neutrons in the slab minus the number absorbed or

$$\text{number leaking out} = 2\ SL\ \frac{\sinh\ (^b/2L)}{\cosh\ (^a/2L)} \tag{8}$$

All the parameters needed to solve this equation are either known or, in the case of a, can be obtained. The value of a is assumed to be

$$a = 2(.71\ \lambda_{tr} + {}^b/2) \tag{9}$$

where (6:131)

$$\lambda_{tr} = \frac{1}{\Sigma_{tr}} = \frac{1}{\Sigma_s\ (1-2/3A)} \tag{10}$$

In the tritium-breeding zones, only those reactions which result in neutron absorption are considered. All absorption cross sections below

1 ev in these zones are inversly dependent of the velocity of the neutron. Since all cross sections have the same functional dependence, the ratios between a macroscopic cross section for a specific absorption reaction and the sum of all the macroscopic cross sections of interest at 1 ev were used to determine the probability for an interaction of a specific type. The Li-6 (n,T) reaction is the predominant reaction in this range, accounting for 99.4% of the reactions. This reaction also makes a significant contribution to the breeding ratio in the thermal range and, since it is an exothermic reaction, it also makes a significant contribution to the heating rate (about 35% of the histories fall below one electron volt). The radiative capture reactions would contribute some heating due to the release of gamma radiation but the rate at which they occur (approximately 2 per 1000 histories) is considered insignificant.

Appendix C - The Rejection Technique

A point of paramount interest in Monte Carlo calculations is the selection of a variable which is distributed according to a given probability distribution. One technique that can be used relys on the inversion of the functional relationship. An example of this technique is discussed in Chapter II, Section C-1 where this technique is used to determine the distance between interactions.

In some cases, this technique is unusable because of the complexity of the functional relationships. In this case, a technique called the rejection technique may be used to advantage. Figure 10 shows a differential distribution function.

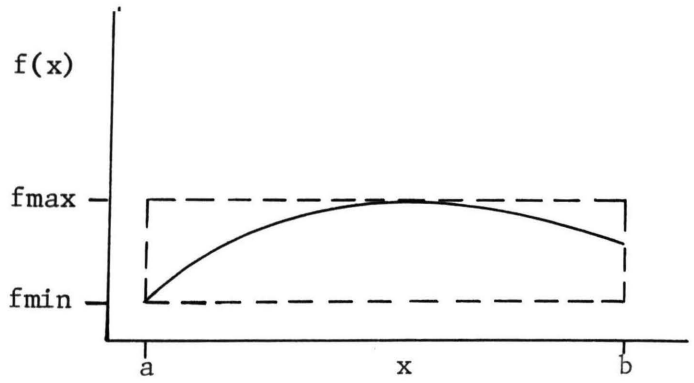

Figure 10 - Differential Distribution Function

The maximum value of f(x) is shown as fmax and the minimum as fmin. For the discussion, we will consider a rectangle bounded by a, b, fmax and fmin with the area in the rectangle being denoted as A. For any given random number ξ, the random numbers

$$S(\xi) = (b-a)\xi + a \qquad (1)$$

$$g(\xi) = (fmax - fmin)\xi + fmin \qquad (2)$$

are uniformly distributed over the intervals a to b and fmin to fmax. (24:246). For any two random numbers ξ_1 and ξ_2, the associated pair $s(\xi_1)$ $g(\xi_2)$ define a point which is randomly distributed over the rectangle. If g >f(s), the point lies above the curve of f(x) and is rejected. Two new random numbers are generated and new values of s, g are determined. Eventually a pair of numbers are found such that g <f(s) in which case the value of s is accepted.

The relative efficiency E with which the value of s is accepted is given by

$$E = {}^{1}/A \qquad (3)$$

The average number of trails needed to find an acceptable value is ${}^{1}/E$. If the area A is large compared to 1, this method is very inefficient and computer time considerations begin to have a bearing.

Appendix D - Model for (n,2n) Reactions

The basic relationships used to develop this model are conservation of energy and momentum. The conservation of momentum equations are:

$$mv = mv' \cos\alpha + MV' \cos\psi \tag{1}$$

$$mv' \sin\alpha = MV' \sin\psi \tag{2}$$

where m and v represent the neutron energy and speed, M and V represent the nuclide energy and speed and α and ψ represent the neutron and nuclide scattering angles respectively in the laboratory system. The primes represent the speed after the interaction. Also, it is assumed throughout that the nucleus is at rest. Using the relationship

$$E = \frac{1}{2} mv^2 \tag{3}$$

and letting m = 1 and M = A, the equations can be written:

$$\sqrt{E_n} = \sqrt{E'_n} \cos\alpha + \sqrt{AE'_a} \cos\psi \tag{4}$$

$$\sqrt{E'_n} \sin\alpha = \sqrt{AE'_a} \sin\psi \tag{5}$$

For the first neutron emitted, the conservation of energy relationship is

$$E_n = E_n' + E'_a + Q \tag{6}$$

where all the E_n, E_n' and E'_a are as defined above and Q is the excitation energy.

Initially, E_n is the only quantity known. In order to determine E_n', the upper and lower limits of E_n' must first be determined. The upper and lower limits, denoted as E' max and E' min, respectively, are determined by solving eqns(4), (5) and (6). The value for E' max is determined by setting $\cos\alpha = 1$ and the value for E' min is determined

by setting $\cos\theta = -1$. The value of $\cos\psi$ is assumed to be equal to 1 in both cases. The Q value used is equal to the binding energy of the least bound neutron, denoted by BE2. This is done because to determine the maximum emergent neutron energy, it must be assumed that only enough excitation energy is given to the nucleus to allow the second neutron to escape. Performing the algebra, one obtains the following values for E' max and E' min:

$$E' \text{ max} = \alpha + \frac{\sqrt{E_n + 2\alpha}}{(A+1)^2} \tag{7}$$

$$E' \text{ min} = \left[\frac{-E_n + \sqrt{E_n + (A+1)\beta}}{A+1}\right]^2 \tag{8}$$

where

$$\alpha = E_n + (A+1) \tag{9}$$

$$\beta = (A-1)\, E_n - A(BE2) \tag{10}$$

With E' max and E' min determined, a quantity denoted here as E'_p can be determined using the evaporation model where the energy is selected from the distribution

$$p(E';) = \frac{E_p' \exp(-E_p'/T)}{N(T)} \tag{11}$$

where T' is the nuclear temperature and N(T) is the normalization factor. A value for E_p' is determined by randomly selecting a value between E' max and E' min and using the rejection technique to determine if the value is acceptable. If it is not, then the process of selection is repeated until an acceptable value is determined. Note that the maximum possible value for E_p' is E max - E min. In order

to determine the value of E'_n, the energy of the emergent neutron, the value determined for E'_p is added to E min.

Using the values E_n and E_n' the value of Q, the excitation energy, can be calculated as follows (6:24)

$$Q = (\frac{A}{(A+1)})m\ [v_e^2 - (\frac{A+1}{A})v_c']^2 \tag{12}$$

where:

$$v_1^2 = \frac{2\ E_n}{m} \tag{13}$$

$$v_o = \frac{1}{A+1}\sqrt{\frac{2\ E_n}{m}} \tag{14}$$

$$v_1' = \sqrt{\frac{2\ E_n'}{m}} \tag{15}$$

$$v_o' = v_o \cos + v_o^2\ (\cos\theta - 1) + (v_e')^2 \tag{16}$$

Here m is the mass of the neutron, E_n is the energy of the incident neutron, v_e is the velocity of the incident neutron in the lab system, v_o is the velocity of the center of mass as observed in the lab system, v_e' is the velocity of the emergent neutron in the lab system and v_c' is the velocity in the CM system. $\cos\theta$ is the cosine of the polar scattering angle in the CM system. In this model, it is assumed that both the polar and the azimuthal angles are isotropic in the CM system. They are picked from the appropriate distribution function prior to determining Q.

The value of the polar scattering angle in the lab system can be determined from the relationship (6:29)

$$\tan\alpha = \frac{\sin\theta}{\gamma+\cos\theta} \tag{17}$$

where gamma is defined as

$$\gamma = \frac{1}{A}\sqrt{\frac{QE_n}{A\,E_n-(A+1)Q}} \tag{18}$$

The determination of the parameters for the second emergent neutron follows essentially the same steps as for the first.

In the case of the second neutron, the energy relationship is

$$E_a+Q = E_n'' + BE2 + E_{A-1} \tag{19}$$

where E_a, Q and BE2 have been previously defined, E_n'' is the energy of the second neutron and E_{A-1} is the energy of the nucleus after the departure of the second neutron.

The maximum and minimum energy are determined the same way as before but this time the results are:

$$E''\,max = [\frac{\alpha+ 2\,E_A\sqrt{1 + (\beta/E_A)}}{A}] \tag{20}$$

$$E''\,min = [\frac{E_A + \sqrt{(A-1)(Q-BE2)}}{A}]^2 \tag{21}$$

In this case, α and β are defined as follows:

$$\alpha = + 2E_A \tag{22}$$

$$\beta = (A-1)(Q-BE2)-E_A \tag{23}$$

The azimuthal scattering angle is again considered to be isotropically distributed in the lab system. The polar angle in the lab system is calculated by using the relationship (10:411)

$$Q = E_n''[1 + \frac{1}{(A-1)}]-E_A[1 - \frac{A}{A-1}]-2\frac{\sqrt{(AE_a)E_n''}}{A-1}\cos\theta \tag{24}$$

In this case, it is assumed that Q equals zero which means that the nucleus retains no excitation energy, only kinetic energy. Solving the equation gives

$$\cos\theta = \frac{A\,E_A + E_n'' = E_{A-1}(A-1)}{2\sqrt{(A\,E_A)(E_n'')}} \tag{25}$$

Use of this relationship insures that momentum is conserved in the system.

Appendix E - Determination of Boundary Crossing Point

The problem of finding the point where a particle track crosses a zone boundary can be defined in geometric terms as the intersection of a directed straight line segment $(x_1, y_1, z_1) \rightarrow (x_2, y_2, z_2)$ with a function of $f(x,y,z)$. In the case of a cylinder, the function is defined as

$$x^2+y^2-J = 0 \tag{1}$$

where J is equal to the value of the zone of interest squared.

For the purpose of the discussion, the following terms are defined:

$$u = x_2-x_1 \tag{2}$$

$$v = y_2-y_1 \tag{3}$$

the line segment can then be defined by

$$\frac{x-x_1}{u} = \frac{y-y_1}{v} = p \mid 0 \leq p \leq 1 \tag{4}$$

or

$$x = up + x_1 \tag{5}$$

$$y = vp + y_1 \tag{6}$$

Substituting the values of eqn(4) and (5) into the equation of the function gives

$$f(p) = (up+x_1)^2+(vp+y_1)^2-J = 0 \tag{7}$$

when eqn(7) is expanded, it can be written as

$$(u^2+v^2)p^2+2p(ux_1+vy_1)+x_1 2+y_1 2+J \tag{8}$$

which can be written as

$$Rp^2+2Qp+F \tag{9}$$

where

$$R = u^2 + v^2 \tag{10}$$

$$2Q = 2ux_1 + 2vy_1 \tag{11}$$

$$F = x_1^2 + y_1^2 - J \tag{12}$$

If R = 0, we have a linear equation with one root

$$p = -F/2Q \tag{13}$$

If R is not equal to zero, then f(0) = F and f(1) = R+2Q+F. If f(0) and f(1) have unlike signs, there is one solution

$$p = \frac{-Q \pm \sqrt{Q^2-RF}}{R} \tag{14}$$

where the radical sign is the sign opposite to that of F (20:94)

If f(0) and f(1) have like signs, then there are either two roots in the interval (0,1) or no roots. Since -Q/R is the mean of the two roots of the equation, the following conditions must be met:

1) Q and R must have unlike signs (15)

2) $|Q| < |R|$ (16)

3) $Q^2-RF>0$ (17)

for real roots. Of the two roots, we want the smaller, so the radical must be given the sign of Q. In order to have the root

$$-Q \pm \frac{\sqrt{Q^2-RF}}{R} > 0 \tag{18}$$

we must have

$$|Q| > \sqrt{Q^2-RF} \tag{19}$$

or R and F must have like signs. Since these conditions guarantee the existence of a solution, they represent the necessary and sufficient conditions for the root (20:45).

When F = 0 (particle is on a boundary), the other root lies at 2Q/R.

$$p = \frac{2Q}{R} \tag{20}$$

Appendix F - Error Analysis

Consider a quantity calculated by

$$\bar{\xi}_n = \frac{1}{N} \sum_{i=1}^{R} \xi_i \tag{1}$$

where ξ_i corresponds to the weight of the i^{th} "success" contributing to the value of $\bar{\xi}_n$, R is the number of successes and N is the number of histories studied. The variance of $\bar{\xi}_n$ is given by (21:18)

$$\sigma^2 = \frac{N}{N-1} \left[\frac{1}{N} \sum_{i=1}^{R} \xi^2_i - \left(\frac{1}{N} \sum_{i=1}^{R} \xi_i\right)^2\right] \tag{2}$$

In the case where the number of specific type of interaction is of interest, ξ_i equals one if the interaction takes place and zero if it does not; hence, R would be equal to the number of interactions of interest that take place during a particular group of histories. In this case where the heating rate is the blanket, it is the item of interest, ξ_i, which represents the energy deposited at a particular location.

The relative error is defined as (22:14)

$$\frac{\Delta \bar{n}}{\bar{n}} = \frac{n^2}{\bar{\xi}_n} \tag{3}$$

where N represents the number of histories, σ^2 is the variance and $\bar{\xi}_n$ is the quantity of interest.

In the case where several parameters contribute to the quantity of interest, e.g., total heating in a zone is equal to the neutron heating plus the gamma heating in that zone, the value for $\Delta\bar{n}$ is computed by the following method (2:14)

$$\Delta \bar{n} = \sum_{i=1}^{R} \frac{i^2}{N} \qquad (4)$$

where $\Delta\bar{n}$, and N are as defined previously and the summation is over all parameters contributing to the error.

226901